

**ELECTRICALLY CONTROLLED RELEASE OF DOPAMINE FROM
NANOPOROUS CONDUCTING POLYMERS**

by

Michael Freedman

University of Pittsburgh, 2010

Submitted to the University of Pittsburgh

Honors College in partial fulfillment

of the requirements for the degree of

Bachelors of Philosophy

University of Pittsburgh

2010

UNIVERSITY OF PITTSBURGH
UNIVERSITY HONORS COLLEGE

This thesis was presented

by

Michael S. Freedman

It was defended on

March 16, 2010

and approved by

Shigeru Amemiya, Chemistry, University of Pittsburgh

Guoqiang Bi, Biophysics and Neurobiology, University of Science and Technology of China

Adrian Michael, Chemistry, University of Pittsburgh

Thesis Director: Xinyan Tracy Cui, Bioengineering, University of Pittsburgh

Copyright © by Michael Freedman

2010

**ELECTRICALLY CONTROLLED RELEASE OF DOPAMINE
FROM NANOPOROUS CONDUCTING POLYMERS**

Michael Freedman, BPhil

University of Pittsburgh, 2010

Conducting polymers are synthesized on electrode surfaces, conduct electricity, and can incorporate different molecules. These properties make them ideal for biocompatible application to interface with the nervous system, particularly for drug release. This thesis describes the development of system based on nanoporous conducting polymers for the controlled release of dopamine. Polypyrrole, a conducting polymer, was demonstrated to release the neurotransmitter dopamine when electrically stimulated. Dopamine release from nanoporous and non-nanoporous polypyrrole films was characterized. Diffusion from unstimulated polypyrrole accounts for much of the dopamine release, while a fraction of the dopamine was released in a controllable fashion when the polypyrrole film was stimulated. Dopamine was retained by holding the releasing electrode at a negative potential. Dopamine release was quantified by fast-scan cyclic voltammetry using carbon-fiber microelectrodes.

Successful controlled release of dopamine from conducting polymer films is promising for treatment of neurological conditions characterized by low dopamine levels, neuroscience research investigating the effects of neurotransmitters on network activity, and it also serves as a model system for controlled release of other similar molecules of pharmaceutical interest.

TABLE OF CONTENTS

PREFACE	xii
1.0 BACKGROUND	1
1.1 Overview	1
1.2 Conducting Polymers	2
1.2.1 Drug Release via Reversible Oxidation-Reduction Reaction	4
1.2.2 Effects of Morphology	6
1.3 Dopamine: Structure and Function	7
1.3.1 Biophysical Properties and Translatability	7
1.3.2 Clinical Applications for Controlled Dopamine Release	11
1.4 Electrochemical Detection of Dopamine	13
1.4.1 Introduction to Electroanalytical Techniques	13
1.4.2 Fast-Scan Cyclic Voltammetry	16
1.4.3 Carbon-Fiber Microelectrodes for Catecholamine Detection	18
1.5 Specific Aims	19
2.0 EXPERIMENTAL	20
2.1 Preparation of Release Electrodes	20
2.2 Electropolymerization of Conducting Polymer Films	21
2.3 Preparation of Carbon-Fiber Microelectrodes	23
2.4 Calibration of Carbon-Fiber Microelectrodes via Fast-Scan Cyclic Voltammetry	23
2.5 Cathodic Binding of Dopamine to Conducting Polymer Films	24
2.6 Electrically Controlled Dopamine Release	24
3.0 RESULTS	28
3.1 Carbon-Fiber Microelectrodes	28

3.1.1 Calibration.....	28
3.1.2 Equilibration	31
3.2 Synthesis and Characterization of PPy/PSS/DA Electrodes.....	34
3.2.1 Electropolymerization of PPy/PSS Films	34
3.2.2 Redox Threshold and Stability of PPy/PSS	35
3.2.3 Cathodic Binding of Dopamine to PPy/PSS Films.....	36
3.3 Effect of Electrical Release Stimulus on FSCV	36
3.4 Controlled Dopamine Release from Flat PPy/PSS Films	37
3.5 Dopamine Release from Uncapped Nanoporous PPy/PSS Films.....	40
3.5.1 Diffusion	40
3.5.2 Electrically Controlled Release.....	42
3.6 Dopamine Release from Capped Nanoporous PPy/PSS.....	43
3.6.1 Diffusion	43
3.6.2 Electrically Controlled Release.....	44
3.7 Summary of Dopamine Release from Polymer Films	45
4.0 DISCUSSION.....	47
4.1 Cathodic Binding of Dopamine	47
4.2 Dopamine Release	49
4.3 Dopamine Release from Capped Nanoporous Films.....	52
4.4 Limitations of Experimental Setup	54
4.5 Limitations with Dopamine	57
5.0 CONCLUSIONS AND FUTURE WORK.....	60
REFERENCES	61

LIST OF EQUATIONS

Equation 1. $O + ne^- \leftrightarrow R$	13
--	----

LIST OF TABLES

Table 1. Common Reference Electrode Potentials and Half Reactions.....	14
--	----

LIST OF FIGURES

Figure 1. Structures of conducting polymers.....	3
Figure 2. Oxidative electropolymerization and doping of PPy (n = the number of Py monomers per dopant molecule, noted as A^-).....	3
Figure 3. Release mechanism for small, mobile dopants of PPy (top), and release mechanism of cationic ions for PPy with large, immobile dopants (bottom). Oxidation is indicated on the left side, and reduction is on the right side (A^- denotes anionic dopant, X^+ denotes cation).....	6
Figure 4. Biosynthesis pathway of catecholamines.....	8
Figure 5. The protonated species (right) is favored in neutral pH.....	9
Figure 6. Interconversion between dopamine and dopamine <i>o</i> -quinone.....	10
Figure 7. Two-electrode (A) and three-electrode (B) electrochemical cells.....	15
Figure 8. Voltage as a function of time in cyclic voltammetry.....	16
Figure 9. A model cyclic voltammogram, showing current as a function of potential. i_{pc} and i_{pa} represent cathodic and anodic peak currents, corresponding to reduction and oxidation, respectively, of the electrochemical species. E_{pc} and E_{pa} represent the potentials at which these peak currents occur.....	17
Figure 10. Background Subtraction. A, B, and C refer to the background signal alone, the background and the analyte signal (dopamine), and the background subtracted curve respectively.....	18
Figure 11. SEM images of (a) the polystyrene nanobead template, (b) the nanoporous PPy film remaining after the nanobeads were dissolved away, (c) the nanoporous PPy film covered with an additional capping layer of PPy, and (d) a cross-sectional image of the interface between the nanoporous PPy (white arrows) and the additional capping layer of PPy (black arrows).....	22
Figure 12. Electropolymerization scheme illustrating preparation of each of the three polymer films. (A) PPy/PSS films are polymerized with constant current at 311 μ A for 100 seconds either through the nanobead template or on the bare GCD electrode surface in a solution of 0.05 M Py and 0.03 M PSS. (B) Polystyrene nanobeads are dissolved by toluene overnight, leaving nanoporous PPy/PSS. (C) PPy/PSS cap is polymerized over nanoporous PPy/PSS via cyclic voltammetry in a solution of 0.05 M Py and 0.03 M PSS.....	22
Figure 13. Evolution of dopamine release experimental configuration.....	27

- Figure 14. Peak currents (nA) of dopamine solutions of known concentrations in 10X PBS as observed in the flow cell as a function of time (s). The maximal peak current generated for each concentration was used for the calibration curve.....28
- Figure 15. Calibration curve for electrochemical detection of dopamine in different solvents (error bars indicate standard error).29
- Figure 16. Calibration curves for electrochemical detection of dopamine displayed across a wide range of concentrations (A) and compared with a linear fit when plotted logarithmically (B).....30
- Figure 17. (A) Dynamic background-subtracted cyclic voltammogram as the CFME equilibrated in 10X PBS. Voltage Point Number (VPN) indicates the potential of the CFME as a function of its point of progression in the voltage sweep. Each cycle is divided into 1000 increments as the voltage sweeps from 0 to +1.0 V, down to -0.5 V, and back to 0 V. (B) Decaying peak current at +0.6 V (VPN ~200), the characteristic oxidation potential of dopamine, from Fig. 17A as the CFME equilibrates over time.....32
- Figure 18. (A) Dynamic background-subtracted cyclic voltammogram after the CFME has equilibrated to steady state. Note the difference in scale of the current (+z) axis between Figures 17A and 18A. (B) Steady-state peak current from Fig. 18A at +0.6 V, the characteristic oxidation potential of dopamine, as a function of time. The current does not exceed ± 2 nA.....33
- Figure 19. Average chronopotentiometric potential curves for electropolymerization of PPy/PSS films on bare GCD electrodes and GCD electrodes with a nanobead template (n=10 per group).....34
- Figure 20. Cyclic voltammogram of flat PPy/PSS film on GCD electrode in 1X PBS solution using a three-electrode setup vs Ag/AgCl reference and platinum wire counter electrodes (scan rate = 100 mV/s). Several cycles are superimposed to depict the change in the response of the PPy/PSS film to repeated charging and discharging.....35
- Figure 21. Amperometric decay as a function of time. Dopamine (0.1 M in deionized water) was cathodically bound to nanoporous PPy/PSS films by applying -0.6 V vs Ag/AgCl to the PPy/PSS modified electrodes for 200 seconds (n=10).....36
- Figure 22. Dynamic peak current of CFME in 10X PBS over time with electrical stimulation. This is the stimulus control for nanoporous and flat PPy/PSS modified electrodes. Stimulation of the GCD electrodes suddenly changes the equilibrium of the solution, resulting in artifacts visible from the FSCV in the form of vertical lines.....37
- Figure 23. (A) Dynamic background-subtracted cyclic voltammogram of pulsatile dopamine release from flat PPy/PSS modified GCD electrodes. Dopamine oxidation was characterized at +0.634 V (VPN ~211), and peak current at this potential was plotted (B). To prepare this electrode, dopamine (0.05 M) was

cathodically bound to PPy/PSS by applying constant voltage of -0.6 V for 100 seconds. Time starts at 400 seconds because the experimental setup was configured as described in Fig. 13A, requiring replacement of the platinum electrode used for background with the PPy/PSS/DA modified GCD electrode.....39

Figure 24. Dynamic background-subtracted cyclic voltammogram illustrating dopamine diffusion over time from a nanoporous PPy/PSS film. Dopamine oxidation peak current is identified by the contour of the maximal red crest, occurring at +0.631 V (VPN ~210). The PPy/PSS modified electrode held at a bias of 0 V vs Ag/AgCl.....40

Figure 25. Peak current at dopamine oxidation potential detecting diffusion of dopamine from uncapped nanoporous PPy/PSS as a function of bias of the GCD electrode (n=1 for 0 V bias, n=2 for -0.3 V bias).....41

Figure 26. Dynamic profiles of dopamine peak currents vs time from nanoporous PPy/PSS films.42

Figure 27. Peak current at dopamine oxidation potential to detect diffusion from nanoporous PPy/PSS films capped with an additional layer of PPy/PSS as a function of time.....44

Figure 28. Change in peak current at dopamine oxidation potential as a function of time for capped nanoporous PPy/PSS film after diffusion. Background current was defined as the current recorded after dopamine diffusion in solution.....45

Figure 29. Dopamine release from the various substrate electrodes via diffusive and controlled release mechanisms. Diffusion from the capped nanoporous film at -0.3 V (not shown) released 1250 ng of dopamine. Error bars indicate standard deviation, sample size is n=1 for both uncapped nanoporous diffusion at 0 V and flat controlled release, and n=2 for both uncapped nanoporous controlled release and uncapped nanoporous diffusion at -0.3 V.....46

PREFACE

It is often said that we are a reflection of the environment in which we live, and I could not agree with this sentiment more strongly. This project would not have been possible without the help of so many people. First and foremost, I would like to thank my thesis advisor, Dr. Tracy Cui. I am humbled and incredibly grateful for her generosity, patience, trust, and confidence in letting me, an undergraduate student, run my own projects. These past four years in her lab have been the foundation for much of my intellectual and personal growth, and I feel extraordinarily lucky to have her for an advisor, mentor and friend.

I would also like to thank the members of my committee: Dr. Guo-qiang Bi, Dr. Shigeru Amemiya, and particularly Dr. Adrian Michael for allowing me to share his lab space and equipment for much of this project. I cannot thank Keith Moquin enough for his help in working through the technical challenges of my experiment and the patience required therein. I also wish to thank the members of the Neural Tissue Engineering Laboratory, especially Dr. William Stauffer and Dr. Xiliang Luo. I am very thankful for the generosity and enthusiasm of the late Dr. G. Alec “Doc” Stewart, the dean of the Honors College. Lastly, I would like to thank my parents and my sisters for their endless love and support. They have always been there for me unconditionally, and continue to help me appreciate the journey over the destination. I am truly grateful.

I acknowledge the financial support of the University Honors College, the Pittsburgh Tissue Engineering Initiative, the University of Pittsburgh Department of

Bioengineering, NSF Grant 0729869 and NSF Career Award DMR-0748001. I thank the Department of Mechanical Engineering and Materials Science for the provision of access to the electron microscopy instrumentation and for assistance with the execution of this part of my research.

1.0 BACKGROUND

1.1 Overview

Advances in smart biomaterials research have made great strides in solving some of the most challenging medical dilemmas. Bioactive conducting polymers are one such area of research that holds great potential. They are synthesized on conductive substrates, are electrically conductive, and their highly customizable properties make them ideal for biomedical applications. Varying the substrate surface and method of synthesis can tailor conducting polymers to have a wide range of morphologies and surface structures. One unique aspect of their mechanism of synthesis is the inherent capability of incorporating different molecules including proteins and drugs, and careful choice of these molecules can customize the polymer for highly specialized bioactivity and increased biocompatibility. Conducting polymers undergo a characteristic charging and discharging of their backbone, and this reversible reaction is ideal for mediating controlled drug release.

My research has been focused on optimizing this mechanism to maximize the capacity and control the release of dopamine from nanoporous conducting polymers. Localized, controlled release of dopamine is highly desirable for the treatment of a range of neurological disorders characterized by low extracellular dopamine concentrations, most notably Parkinson's disease. The development of a conducting polymer system to release dopamine in a controllable fashion has applications for the release of a variety of drugs that share similar chemical properties.

1.2 Conducting Polymers

Conducting polymers are large macromolecules characterized by monomeric units connected by a conjugated backbone. This backbone is comprised of atoms with parallel p orbitals, constituting a delocalized pi system across which electrons can flow freely. This class of polymers includes polyacetylenes, polyanilines, polythiophenes, and polypyrroles (Figure 1). Polymerization can occur via either chemical or electrochemical mechanisms [1]. Electropolymerization has many advantages over chemical synthesis pathways, including ease of synthesis, customizability, and polymer synthesis directly on the conductive surfaces of electrodes.

Polypyrrole (PPy) is the conducting polymer of interest in this thesis and its mechanism of electropolymerization has been studied extensively [2, 3]. When an oxidative potential is applied to pyrrole (Py) monomers in solution, the monomer will undergo oxidation to a delocalized radical cation. This is followed by radical coupling dimerization and further oxidative polymerization until the oligomer exceeds a critical length, loses solubility in solution, and deposits on the anode. Once this occurs, polymerization at the anode surface occurs more easily and at lower potential, and negatively charged counterions called dopants are incorporated into the polymer film to balance the positive charge on the PPy backbone [1-4]. During these simultaneous processes of electrochemical synthesis and polymer doping, the amount of dopant incorporated can range between 30 – 50% of the total weight of the polymer film [1, 2]. The simplified electropolymerization and doping mechanism is illustrated in Figure 2, and outlined in detail by John and Wallace [3].

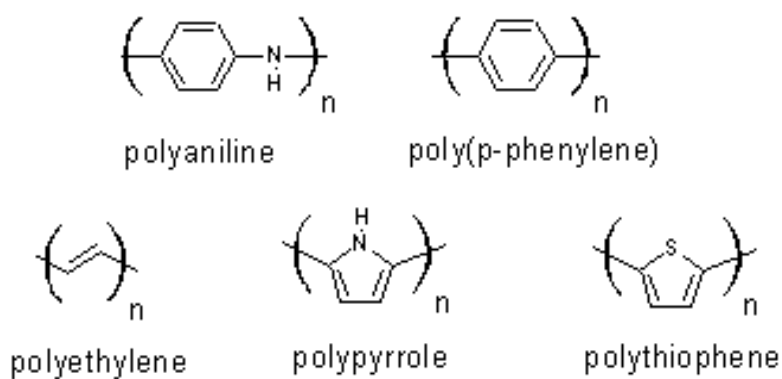


Figure 1. Structures of conducting polymers.

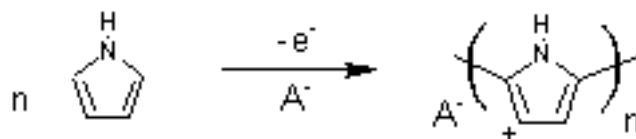


Figure 2. Oxidative electropolymerization and doping of PPy (n = the number of Py monomers per dopant molecule, noted as A^-).

Choice of dopant molecule has profound effects on the adaptability of the resulting polymer film, especially for biomedical applications [5-16]. One particularly appealing development has been the incorporation, both irreversible and reversible, of large biomolecules as dopants in conducting polymer films to optimize their bioactivity for specific functions. In this regard, conducting polymer films have been doped with heparin [5, 6], hyaluronan [7], silk-like polymer with fibronectin fragments, and peptide sequences from laminin [8, 9]. Integration of biomolecules into conducting polymer films does not compromise their biophysical functionality or the electrically active properties of the polymer.

The properties of conducting polymers that make them highly attractive candidates for biomedical applications are not limited to their capacity for customizability. Conducting polymers such as PPy have been shown to have excellent inherent biocompatibility, low electrical impedance, and as the name suggests, the ability to conduct electricity [7, 10-14]. These characteristics and their ease of synthesis on electrodes make conducting polymers ideal for integration with the nervous system. Past studies have integrated brain-derived neurotrophic factor (BDNF) and neurotrophin-3 (NT-3) in conducting polymer films to preserve spiral ganglion neurons after hearing loss [15-17].

1.2.1 Drug Release via Reversible Oxidation-Reduction Reaction

One of the most attractive properties of conducting polymers for biomedical applications stems from their reversible oxidation-reduction (redox) reaction. Upon electrical stimulation, the polymer is oxidized (loses electrons) or reduced (gains electrons) and the backbone becomes charged or neutral (Figure 3). Subsequently, ions flow into or out of the polymer film to maintain electrostatic charge balance [1]. The ionic flux is accompanied by changes in volume of the polymer as it expands and contracts [10].

The PPy redox reaction drives several processes. In the case of small, mobile anionic dopants, the discharge of the polymer backbone during reduction causes the electrical association between the polymer and the anionic doping molecules to be broken, and the dopant molecules will be released. The ultimate result is controlled release of the dopant molecules through electrical stimulation of the polymer [18]. This

mechanism of anionic dopant release is well studied, and a wide variety of compounds with different clinical applications have been released from PPy films in this fashion. They range from fluorescein and $\text{Fe}(\text{CN})_6^{4-}$ [19-21] to glutamate [21], CNQX [4], salicylate, naproxen [22], ATP [23, 24], and dexamethasone [18]. The mechanism that drives this release is detailed below (Figure 3, top).

The polymer redox reaction also drives motion of cations [1, 25-27]. When the polymer is doped with a large, polyanionic dopant such as polystyrene-sulfonate (PSS), the dopant cannot leave the polymer film when the backbone is reduced due to its large size and intricate integration with the polymer. As a result, cations from the solution are incorporated into the polymer to balance the negative charge of the polyanion. This step is referred to as binding the cation to the polymer film. Oxidation of the polymer then allows the cation to be released into solution [1]. By this mechanism, release of cationic compounds can also be controlled by the application of electrical stimuli to the polymer film. Cationic release has been demonstrated for chlorpromazine, dimethyldopamine, and dopamine, all of which bear positive charge [25-27]. This release mechanism is the underlying process that makes the research presented in this thesis possible.

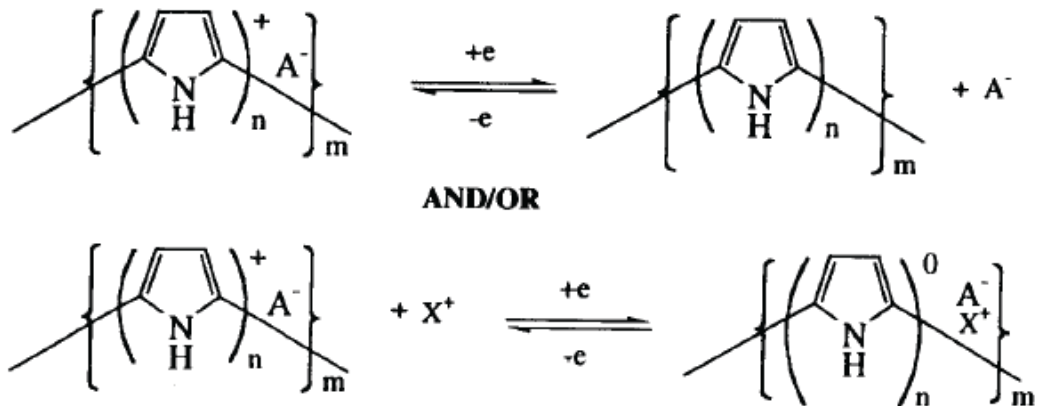


Figure 3. Release mechanism for small, mobile dopants of PPy (top), and release mechanism of cationic ions for PPy with large, immobile dopants (bottom). Oxidation is indicated on the left side, and reduction is on the right side (A^- denotes anionic dopant, X^+ denotes cation). Adapted from [1].

1.2.2 Effects of Morphology

Properties of conducting polymers are heavily influenced by surface morphology. Rougher polymer films increase the available surface area to interface with nervous tissue *in vivo*. This results in a decrease in impedance combined with a more intimate contact between the electrode and surrounding neural tissue, both of which are highly desirable for improving electrode performance in neural recording applications [14]. Changes in polymer structural morphology can also greatly affect drug release processes. When the underlying substrate electrode morphology exhibits increased surface roughness and high surface area, there is an increase in drug load per area and drug is more efficiently released for a given electrical stimulus [28]. Nanoscale structures based on the concept of a drug reservoir, such as nanotubes and nanopores, have also been studied as ways of increasing drug capacity and improving the controllability of release from conducting polymer films [10, 19, 29]. Nanoporous structures are the focus of investigation in this

thesis due to the increased drug capacity afforded by a nanoporous structure. Additionally, a semi-permeable polymer cap could add further controllability to prevent diffusion [19, 29].

1.3 Dopamine: Structure and Function

1.3.1 Biophysical Properties and Translatability

Dopamine is an important neurotransmitter with a variety of functions in the body. In the central nervous system (CNS), it is synthesized by dopaminergic neurons, most prevalent in the substantia nigra and ventral tegmental area within the mesencephalon, as well as the hypothalamus within the diencephalon [30, 31]. As a modulatory CNS neurotransmitter, dopamine is involved in neural mediation of a range of system functions including motor control, emotional regulation, reward, motivation, cognition and endocrine function [32]. In the hypothalamus, dopamine is a neurohormone that serves to regulate pituitary hormones such as prolactin, vasopressin, and oxytocin [33, 34] and has also been connected to regulation of food intake [35]. Dopamine is also synthesized in the adrenal medulla, where it serves as a precursor in the synthesis of the hormones norepinephrine and epinephrine (adrenaline). The biosynthesis pathway of dopamine, as depicted in Figure 4, is extremely well studied. It is synthesized from the amino acid tyrosine which forms its precursor L-3,4-dihydroxyphenylalanine (L-DOPA) [32].

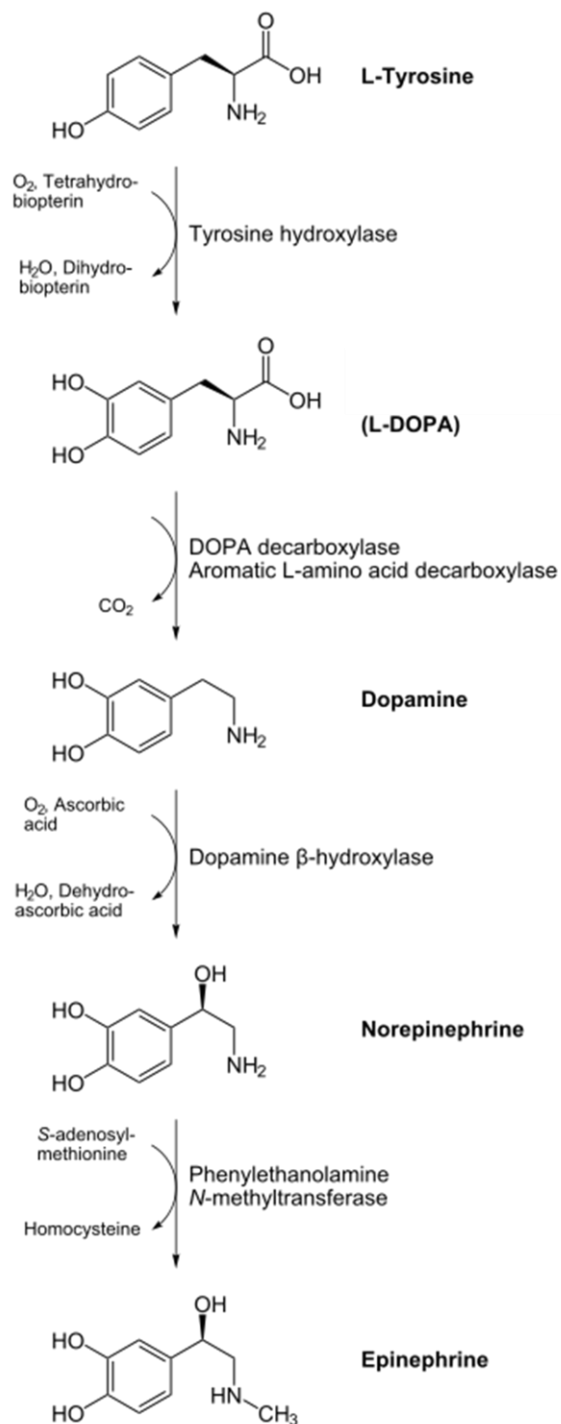


Figure 4. Biosynthesis pathway of catecholamines. Adapted from [36].

Dopamine is classified as a primary monoamine within a category of compounds known as catecholamines. Catecholamines are characterized by a molecular structure that includes a 1,2-dihydroxybenzene ring, an ethyl chain and a terminal amine group. Dopamine, norepinephrine, and epinephrine share these structural characteristics. In pH neutral solution (~7.4), the primary amine group on dopamine favors protonation, yielding a species bearing positive charge (Figure 5) [37, 38]. Its small cationic structure outlines dopamine as a candidate for controlled release from conducting polymers via the cationic release mechanism (Figure 3, bottom).

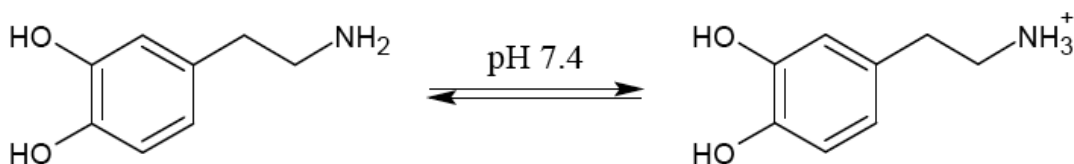


Figure 5. The protonated species (right) is favored in neutral pH.

One characteristic reaction of dopamine and other catecholamines is their ability to undergo autoxidation. In this reaction, dopamine reacts with molecular oxygen in solution or *in vivo* to form *o*-semiquinones and quinones, ultimately ending in polymerization and aggregation of insoluble melanins [39-42]. These mechanisms are mapped in great detail by Graham et al [43]. Dopamine undergoes autoxidation the most rapidly of the catecholamines in question [39]. In tissue, this radical oxidation is thought to have cytotoxic effects [39, 44]. In spectrophotometric quantification of dopamine *in vitro*, autoxidation causes the solution to darken as dopachrome compounds polymerize [40]. This greatly alters the observed absorption spectrum over time, rendering

spectrophotometric methods of dopamine quantification to be of little value. The oxidation of dopamine into dopamine *o*-quinone can be simplified to a two-electron transfer mechanism (Figure 6).

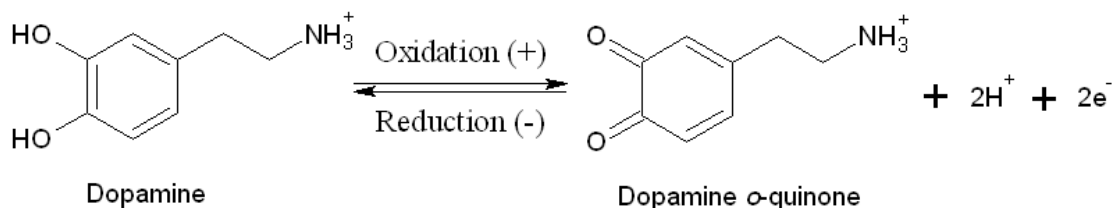


Figure 6. Interconversion between dopamine and dopamine *o*-quinone.

While the oxidation of dopamine to the quinone and subsequent polymerization reactions are undesirable for both *in vivo* cytotoxic effects and *in vitro* spectrophotometric quantification, the initial reversible mechanism has a characteristic electrochemical signature that makes it ideal for electrochemical detection. Electroanalytical methods of dopamine characterization will be discussed in further detail in section 1.4.

As a small positively charged molecule, dopamine is similar in structure to a wide class of catecholamines. Controlled release of molecules such as epinephrine, norepinephrine, and other catecholamines could also potentially be mediated by the same mechanism via conducting polymers, opening a window of new treatment options for diseases influenced by catecholaminergic pathways. Quaternary ammonium salts are another class of small biologically active molecules that bear positive charge, the most well known of which is the neurotransmitter acetylcholine. Thus, application of an

electrically controlled system to release acetylcholine could have profound implications for treatment of Alzheimer's disease, myasthenia gravis, and other diseases affected by cholinergic processes of the nervous system. Subsequently, successful binding and release of dopamine from conducting polymer films serve as a model system applicable to a very large range of pharmaceutically relevant drugs.

1.3.2 Clinical Applications for Controlled Dopamine Release

Many neurological disorders are linked to reduced dopaminergic activity in the central nervous system. For example, affective disorders such as depression have been linked to reduced dopamine turnover and transmission [32, 45, 46]. Dopamine deficiency in the pathology of epilepsy and Parkinson's disease has also been studied extensively. Parkinsonian neurodegeneration is characterized by the loss of dopaminergic neurons in the substantia nigra, and results in significant reductions in extracellular dopamine in the striatum, the region to which these neurons normally project [47]. Additionally, hypoactivity of striatal dopamine is thought to contribute to the development of epilepsy (epileptogenesis), and a substantial amount of research supports the hypothesis of that dopamine has substantial antiepileptic properties [48].

The primary treatment option for patients diagnosed with Parkinson's disease is systemic administration of levodopa (L-DOPA) [49]. Levodopa is capable of crossing the blood-brain barrier, a highly selective barrier that separates blood in the systemic circulation from the cerebral spinal fluid of the central nervous system. Therefore, peripherally administered levodopa can circulate through the bloodstream and cross into the CNS. As a metabolic precursor to dopamine (Figure 4), levodopa in the CNS is

metabolized to dopamine, thereby replenishing dopamine stores in the brain [50]. While there is evidence that levodopa either slows the progression of Parkinson's disease overall or slows the exacerbation of symptoms, there are a multitude of undesirable effects of long-term levodopa treatment [51]. Common adverse side effects include increased dyskinesia, hypertonia, infection, headache, and most prominently, hypotension and nausea [50, 51]. Chronic levodopa treatment can also reduce the effectiveness of individual doses, as well as lead to motor complications due to altered firing patterns of neurons in the basal ganglia [49].

Deep brain stimulation (DBS) is another clinical treatment option for both patients with Parkinson's disease and patients with epilepsy. In deep brain stimulation, electrodes connected to a stimulation apparatus are surgically implanted in the brain. They chronically stimulate either the subthalamic nucleus (STN) or the internal globus pallidus (GPi) at frequencies from 30 – 60 Hz [52, 53]. In patients with Parkinson's disease, DBS has been shown to drastically improve motor symptoms, speech, and overall quality of life while reducing the need for dopaminergic treatment [52]. While the mechanism by which DBS accomplishes these improvements is unknown, therapeutic benefits are also afforded to epileptic patients undergoing DBS treatment including substantial reduction in seizing [53, 54].

Electrically controlled dopamine release is potentially another avenue of treatment of neurological disorders characterized by reduced dopaminergic activity. Conducting polymer based release systems are synthesized directly on electrode surfaces, making integration with pre-existing DBS apparatuses highly feasible. Localized delivery of dopamine from an electrode implanted in the nervous tissue of the brain also

eliminates the need for systemic administration of levodopa, thereby reducing undesirable effects while still achieving the clinical goal of replenishing depleted dopamine levels.

1.4 Electrochemical Detection of Dopamine

1.4.1 Introduction to Electroanalytical Techniques

The field of electrochemistry can be defined very broadly, describing any process that involves the transfer of electrons. This ranges from the corrosion of metal, batteries powering electrical devices, and industrial processes such as electroplating. The fundamental relationship of electron transfer in oxidation-reduction (redox) reactions is described by a half reaction:



The oxidized species (O) and the reduced species (R) differ by n electrons (Equation 1). Each half reaction has a characteristic potential (voltage) at which this reaction occurs. In electrochemical systems, two half reactions occurring at separate electrodes are linked together, and they respond to the potential difference at the electrode - electrolyte interface. Interest is typically focused on one of these half reactions, occurring at an electrode called the working electrode. The potential of the working electrode must therefore be normalized by the known potential of the other half reaction occurring at an electrode called the reference electrode [55]. The international standard for reference potential of electrochemical cells is characterized by the half reaction of $2H^{+}$ reducing to diatomic hydrogen occurring at a normal hydrogen electrode (NHE), but other reference

electrodes such as silver-silver chloride (Ag/AgCl) and saturated calomel electrodes (SCE) are common (Table 1) [55].

Table 1. Common Reference Electrode Potentials and Half Reactions.

Reference Electrode	Reaction	Potential (V)
NHE	$2\text{H}^+ + 2\text{e}^- \leftrightarrow \text{H}_2$	0
SCE	$\text{Hg}_2\text{Cl}_2 + 2\text{e}^- \leftrightarrow 2\text{Hg} + 2\text{Cl}^-$	0.242 (in Saturated KCl)
Ag/AgCl	$\text{AgCl} + \text{e}^- \leftrightarrow \text{Ag} + \text{Cl}^-$	0.197 (in Saturated KCl)

Applying a potential to the working electrode generates a response within the electrochemical cell called a current. In electrochemical systems, this flow of electrons exists as either faradaic or non-faradaic current. Faradaic current describes the physical transfer of electrons between the electrode and a species in solution, whereas non-faradaic current describes all other processes that can occur with a change in potential and cause a transient flow of current, including adsorption/desorption and capacitive charging of the electrical double layer (adsorbed solvent molecules and ions). Direct measurement of faradaic current is a useful electroanalytical tool to study redox reactions, while non-faradaic (capacitive) current contributes to the background signal.

The two conventional setups of electrochemical cells are two-electrode and three-electrode configurations and are used in different circumstances. The two-electrode configuration consists of the working electrode and the reference electrode. Current flows between the two electrodes, and voltage is measured across them. This is used in solutions with less resistance, and can be used in highly resistive solutions with a microelectrode as the working electrode (Figure 7A). Three-electrode systems include an

auxiliary (or counter) electrode as well, and are typically for systems with high solution resistance. In this setup, current flows between the working and auxiliary electrodes, but voltage is measured across the reference and working electrodes (Figure 7B). Three electrodes also allow for improved control of potential between the reference and the working electrodes by removing the reference electrode from the current loop [56].

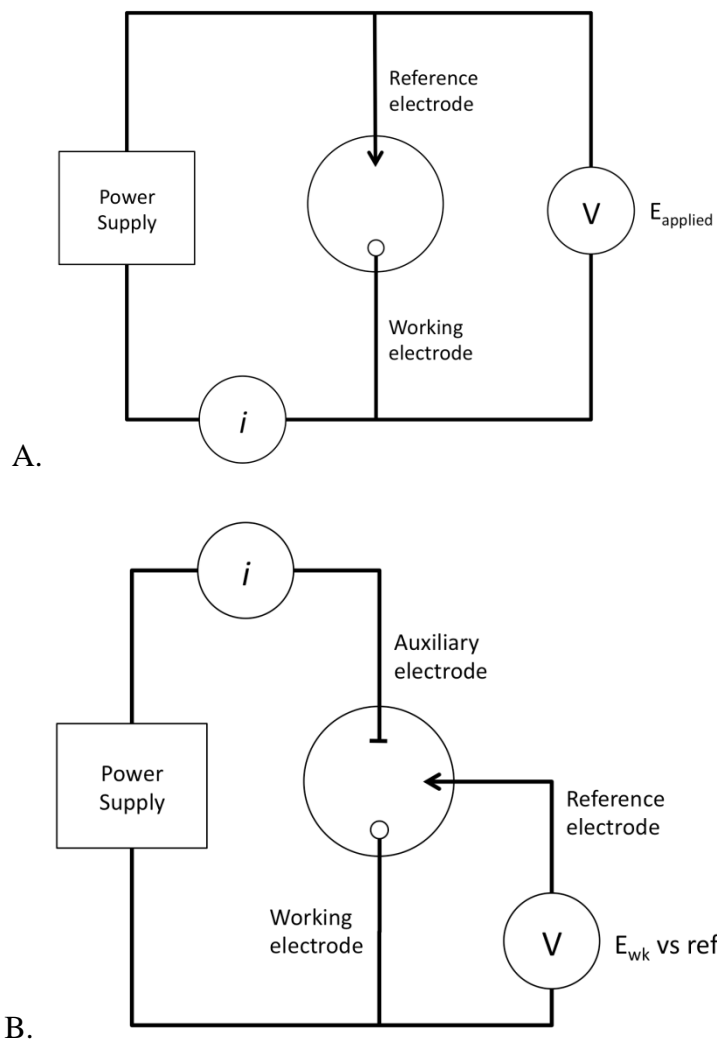


Figure 7. Two-electrode (A) and three-electrode (B) electrochemical cells [55].

1.4.2 Fast-Scan Cyclic Voltammetry

Cyclic voltammetry is a powerful analytical tool used for a variety of purposes. It has been used extensively to identify and quantify concentrations of biologically important analytes. In this process, the potential of the working electrode is linearly ramped above the oxidation potential and below the reduction potential of the analyte of interest, and the resulting current is recorded (Figure 8). When the potential applied is sufficient to drive the transition of the analyte to the oxidized or reduced state, the current is proportional to the number of molecules electrolyzed [57]. The results of cyclic voltammetry are displayed graphically in a cyclic voltammogram, with current as a function of potential applied (Figure 9). The maximal current at the potential of oxidation or reduction is called the peak current (i_p).

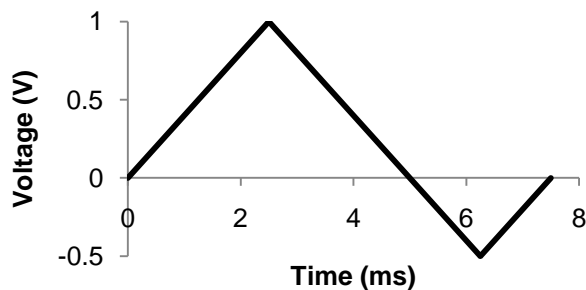


Figure 8. Voltage as a function of time in cyclic voltammetry.

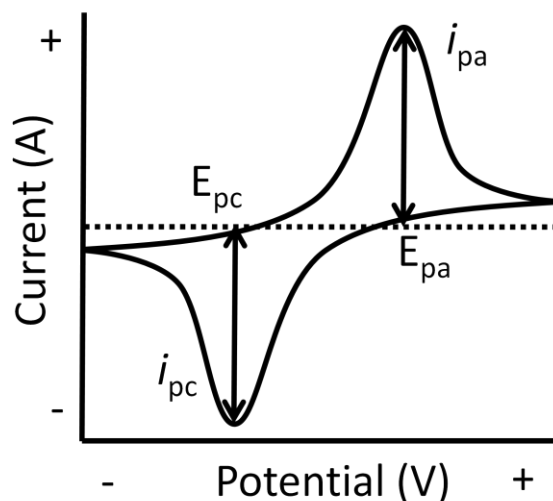


Figure 9. A model cyclic voltammogram, showing current as a function of potential. i_{pc} and i_{pa} represent cathodic and anodic peak currents, corresponding to reduction and oxidation, respectively, of the electrochemical species. E_{pc} and E_{pa} represent the potentials at which these peak currents occur.

The rate at which the potential is swept is called the scan rate (v), and can profoundly affect the cyclic voltammogram. Cyclic voltammetry performed at high scan rates is called fast-scan cyclic voltammetry (FSCV). The relationship between peak current and scan rate depends on the geometry of the electrode, the subsequent mode of transport that dominates, and structure of the electrode-electrolyte interface. For example, i_p is linear with respect to v for a thin layer of adsorbed species [58], while it is linear with respect to $v^{1/2}$ for linear diffusion-mediated processes at planar electrodes [55]. Additionally, though the peak current, i_p , indicates the faradaic current from the oxidation of the analyte of interest, the total current is the sum of faradaic (redox) and non-faradaic (capacitive charging) currents. In cyclic voltammetry, the non-faradaic current is proportional to the scan rate [55]. Therefore, as scan rate increases, the background current gets substantially larger. The conventional method for eliminating this

background signal is called background subtraction (Figure 10). A cyclic voltammogram is acquired in the solvent without the analyte of interest, and the current of this voltammogram is subtracted from subsequent cyclic voltammograms that contain the peak current of the oxidized (or reduced) analyte.

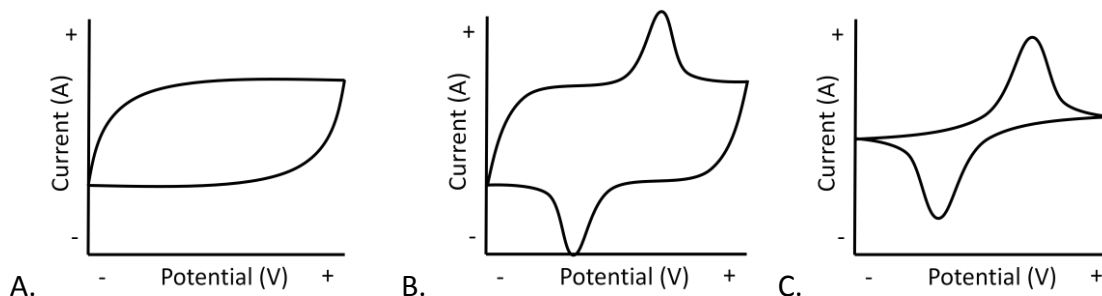


Figure 10. Background Subtraction. A, B, and C refer to the background signal alone, the background and the analyte signal (dopamine), and the background subtracted curve respectively.

1.4.3 Carbon-Fiber Microelectrodes for Catecholamine Detection

Reduction of the size of electrodes used in voltammetric processes dramatically improves the quality of electrochemical data. Microelectrodes have much larger current density than larger electrodes because of radial and perpendicular diffusion. Fast-scan cyclic voltammetry can reduce the contribution of capacitive (non-faradaic) current at microelectrodes, but background subtraction is still useful [55, 59]. The small double-layer capacitance of microelectrodes allows the potential of the electrode to change rapidly. When used in conjunction with FSCV, microelectrodes can achieve very high spatial resolution that is ideal for quantifying dynamic changes of catecholamines [60].

Sensitivity and selectivity of FSCV using microelectrodes can be further improved with digital filtering and ensemble averaging processes [61, 62].

1.5 Specific Aims

This investigation has several specific aims for the development of a conducting polymer based dopamine release system:

- (1) To bind dopamine to conducting polymer film
- (2) To release dopamine in a controllable fashion upon application of an electrical stimulus
- (3) To maximize dopamine capacity of conducting polymer film by implementing a nanoporous structure
- (4) To minimize diffusion of dopamine from conducting polymer film by incorporating a semi-permeable cap
- (5) To retain molecular structure and therefore preserve biological functionality of dopamine released from conducting polymer film

The following sections describe in detail how each of these specific aims is approached and the strategies, experimental techniques, and evaluation methods implemented in their execution.

2.0 EXPERIMENTAL

2.1 Preparation of Release Electrodes

Glassy carbon disk (GCD) electrodes (3 mm diameter, 6 mm outer diameter including teflon insulating sheath, CH Instruments) were roughened with fine sandpaper and polished sequentially with 1.0 μm and 0.05 μm alumina slurries. They were then ultrasonically washed with water and ethanol for 5 minutes. The GCD electrodes were then set aside for non-nanoporous (i.e. flat) conducting polymer films as described in the next section, or pretreated electrochemically to make the surface more hydrophilic for the process of synthesizing nanoporous conducting polymer films. Electrochemical pretreatment of GCD electrodes consisted of chronoamperometry (constant voltage) at -1.8V for 200 seconds, followed by five cycles of cyclic voltammetry between 0.3 and 1.3 V at a scan rate of 100 mV/s in a solution of phosphate buffered saline (PBS). This process oxidizes the surface of the GCD electrodes, making them more hydrophilic.

Following electrochemical pretreatment, 5.0 μL of a 1.0% (w/v) polystyrene nanobead suspension (mean diameter 46 ± 2.0 nm, Duke Scientific) was pipetted onto the GCD electrode surface. The nanobeads serve as a template through which the conducting polymer film will polymerize. The GCD electrodes were placed vertically to dry. When completely dry, the GCD electrodes with the polystyrene nanobead template were heated at 60°C for 15 minutes and then set aside to cool to room temperature.

All electrochemical preparations of GCD electrodes were performed on a Gamry Potentiostat, FAS2/Femtostat (Gamry Instruments) with Gamry Framework software. A three-electrode setup was used with the GCD electrode as the working electrode, a

platinum wire counter electrode and a silver/silver chloride (Ag/AgCl) reference electrode containing 1.0 M KCl.

2.2 Electropolymerization of Conducting Polymer Films

Conductive PPy films were electrochemically synthesized on either flat GCD electrodes or GCD electrodes modified with the polystyrene nanobead template. For electropolymerization, GCD electrodes with or without the nanobead template were immersed in a solution of 0.05 M pyrrole (98%, Sigma-Aldrich, vacuum distilled), 0.03 M poly(sodium styrene-4-sulfonate) (PSS) in deionized water. Using the same three-electrode setup described in the previous section, constant current of 311 μA was applied for 100 seconds to each of the GCD electrodes (Figure 18).

The PPy/PSS films synthesized through the nanobead template were then rinsed with deionized water and left in toluene overnight to dissolve the polystyrene nanobeads, leaving a nanoporous structure. Some of these GCD electrodes modified with nanoporous PPy/PSS were further modified with a semi-permeable conducting polymer “cap” intended to prevent diffusion of DA from the nanoporous film. The cap was electropolymerized via cyclic voltammetry starting at 1.0 V and sweeping between 0.5 V and 1.2 V at a scan rate of 25 mV/s employing the same three-electrode setup. Scanning electron micrograph (SEM) images included below show examples of the microstructure of each of the stages of synthesis of similarly prepared capped nanoporous PPy films (Figure 11) [29]. The final resulting groups of modified GCD electrodes used include those modified with flat PPy/PSS, nanoporous PPy/PSS, and capped nanoporous PPy/PSS films, schematically illustrated in Figure 12.

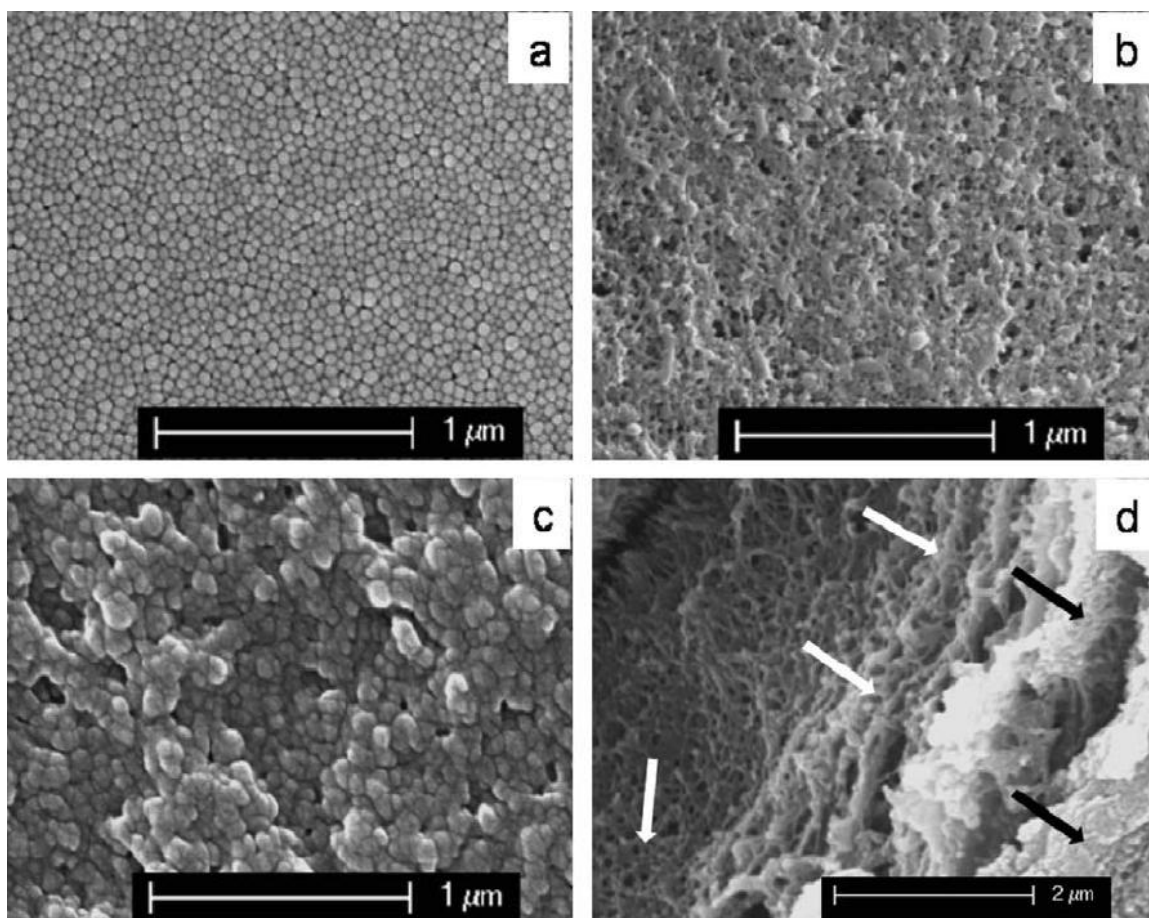


Figure 11. SEM images of (a) the polystyrene nanobead template, (b) the nanoporous PPy film remaining after the nanobeads were dissolved away, (c) the nanoporous PPy film covered with an additional capping layer of PPy, and (d) a cross-sectional image of the interface between the nanoporous PPy (white arrows) and the additional capping layer of PPy (black arrows) [29].

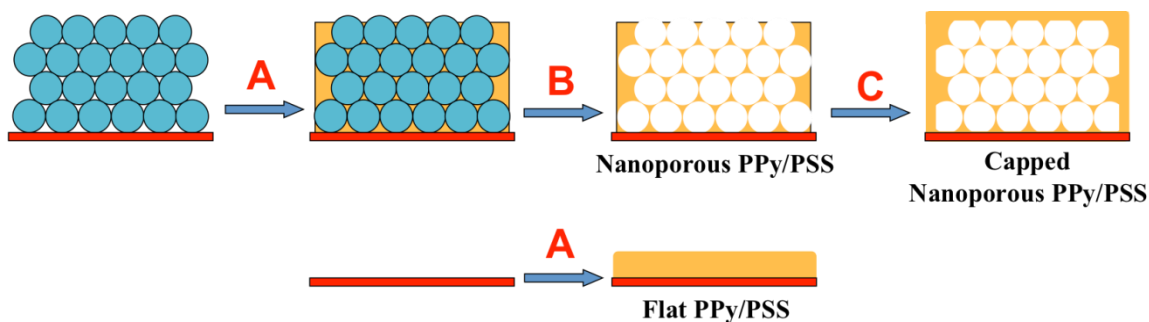


Figure 12. Electropolymerization scheme illustrating preparation of each of the three polymer films. (A) PPy/PSS films are polymerized with constant current at 311 μA for 100 seconds either through the nanobead template or on the bare GCD electrode surface in a solution of 0.05 M Py and 0.03 M PSS. (B) Polystyrene nanobeads are dissolved by toluene overnight, leaving nanoporous PPy/PSS. (C) PPy/PSS cap is polymerized over nanoporous PPy/PSS via cyclic voltammetry in a solution of 0.05 M Py and 0.03 M PSS.

2.3 Preparation of Carbon-Fiber Microelectrodes

Carbon-fiber microelectrodes (CFMEs) were constructed from single 7 μm diameter carbon fibers (T650, Cytec Carbon Fibers LLC) threaded through borosilicate capillary tubes (0.75 mm inner diameter, 1.0 mm outer diameter, A-M Systems, Inc). The capillary tubes were pulled to a fine point around the carbon fiber using a vertical micropipette puller (Narishige) and injected with epoxy (Spurr Epoxy, Polysciences Inc) to fix the position of the fiber. The protruding fiber was trimmed to 400 μm , and the capillary was filled with mercury (electronic grade, Sigma-Aldrich) to bridge electrical contact between the carbon fiber and the tungsten contact wire. CFMEs were sonicated in reagent grade isopropanol (Sigma-Aldrich) containing activated carbon (Fisher Scientific) for 5 minutes prior to use.

2.4 Calibration of Carbon-Fiber Microelectrodes via Fast-Scan Cyclic Voltammetry

CFMEs were calibrated prior to dopamine release. Precalibration serves a dual purpose. First, it establishes a relationship between dopamine concentration and peak current of the cyclic voltammogram. Additionally, pre-exposing the CFME to dopamine prior to the release studies allowed dopamine to adsorb to the CFME to a certain degree and thereby minimizing dynamic changes in the sensitivity of the CFME to subsequent dopamine adsorption in the release experiments. This is explained in further detail in section 3.1. Calibration was performed in a flow cell with gravity-driven concentrated 10X PBS (154 mM NaCl, 100 mM Na_2HPO_4 , titrated to pH ~ 7.4 with NaH_2PO_4). Standard solutions for calibration were prepared with dopamine HCl (Sigma-Aldrich).

Fast-scan cyclic voltammetry (FSCV) was carried out using an EI 400 high-speed bipotentiostat (Ensmann Instruments) and the CV Tar Heels v4.3 software package (Dr. Michael Heien, Department of Chemistry, Pennsylvania State University). The CFME was held at a resting potential of 0 V vs Ag/AgCl reference in a two electrode setup, and the potential was swept to +1 V, down to -0.5 V, and back to 0 V at a scan rate of 400 V/s. Characteristic dopamine oxidation current peaks were observed at $\sim +0.6$ V, and dopamine voltammograms were obtained by background subtraction and sampled at 10 Hz [63].

2.5 Cathodic Binding of Dopamine to Conducting Polymer Films

Dopamine was cathodically bound to the PPy/PSS modified GCD electrodes using the EI 400 bipotentiostat. The PPy/PSS modified electrodes were held at -0.6 V vs Ag/AgCl reference electrode and a platinum rod counter electrode for 200 seconds using a three-electrode setup in a solution of 0.1 M dopamine HCl (Sigma-Aldrich) in deionized water. The resulting polymer film consists of PPy doped with PSS and cathodically bound with dopamine, notated PPy/PSS/DA. The dopamine binding mechanism is thoroughly described in section 1.2.1.

2.6 Electrically Controlled Dopamine Release

Dopamine release from various PPy/PSS films was attempted using a number of experimental setups (Figure 4). All setups were performed with the EI 400 bipotentiostat running two channels simultaneously against Ag/AgCl reference electrode and platinum rod counter electrode in a four-electrode setup (two overlapping three-electrode setups).

The CFME was connected to channel A, constantly running the FSCV waveform as described in section 2.4, whereas channel B controlled the potential of the GCD electrode modified with PPy/PSS/DA. The CFME equilibrated in solution until peak current at DA oxidation potential remained stable within ± 2 nA. The potential of channel B was toggled between -0.3 V, 0 V and +0.3 V vs Ag/AgCl, providing the electrical stimulus that drives the controlled release of dopamine from the PPy/PSS/DA films.

Due to the setup of the initial configuration, the CFME was initially positioned opposite an unmodified platinum disk electrode. The CFME sampled a background current from the PBS solution, and then the platinum disk electrode was replaced with the GCD electrode modified with PPy/PSS/DA (Figure 13A). This was done to avoid acquiring a background signal that contained peaks from dopamine leaking out of the PPy/PSS/DA film, which was observed several times. The undesirable net effect would be background subtraction of a signal that contained the dopamine electrochemical signature as well as the background current, misrepresenting the rest of the release profile. The CFME was positioned 250 μm above the surface of the PPy/PSS/DA film, and the electrochemical experiments were performed in 100 μL of 1X PBS using Ag/AgCl wire as a reference electrode. However, peak currents were observed at inconsistent potentials, leading to a revision in the experimental configuration.

The revised experimental configuration (Figure 13B) included several major changes from the initial setup. To resolve the issue of shifting potentials of peak current, a stronger buffer solution, 10X PBS, was used in place of the original 1X PBS, and the Ag/AgCl wire reference electrode was replaced with a Ag/AgCl reference electrode in an ion-selective membrane containing 10X PBS solution. The revised setup was carried out

in a 200 μ L droplet on a glass substrate, and required the CFME to be fixed to the side of the GCD electrode, greatly increasing the distance between the two electrodes to at least 2.4 mm. This therefore required more time to observe DA release after each stimulus. Additionally, while this configuration allowed CFME equilibration and theoretically acquisition of a DA-free background signal, DA was still observed in the equilibration profile. These suggest that the experimental configuration required further revision.

The final experimental configuration (Figure 13C) separated the CFME and the modified GCD electrode to independent micromanipulators. This allowed the CFME to fully equilibrate and acquire a pristine background signal before the modified GCD was introduced into the system. The modified GCD electrodes were positioned approximately 1 mm away from the CFME.

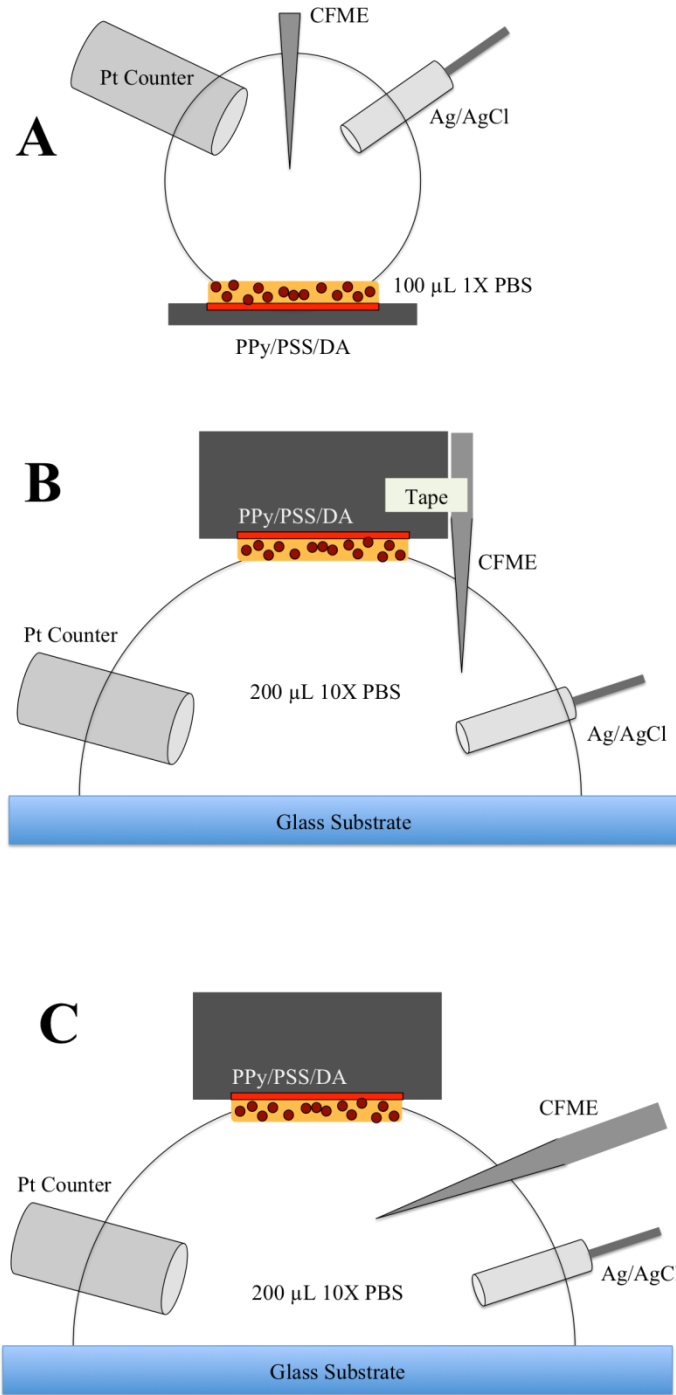


Figure 13. Evolution of dopamine release experimental configuration

3.0 RESULTS

3.1 Carbon-Fiber Microelectrodes

3.1.1 Calibration

Standard solutions of 0.5, 1.0, and 5.0 μM in either 1X PBS or 10X PBS were used to calibrate the CFMEs (Figure 14). Direct correlation was established between dopamine concentration and background subtracted peak current, and there was limited variability between the calibrations of different electrodes. Differences in electrode calibration curves were observed between CFMEs calibrated in different solvents (Figure 15). While the vast majority of CFME calibrations were done in 10X PBS, calibration curves from data obtained in CFME calibrations in other solvents (ACSF = artificial cerebrospinal fluid) are included for comparison. Calibration curves were also obtained for a wider range of concentrations of dopamine, varying from 0.1 μM to 30 μM (Figure 16).

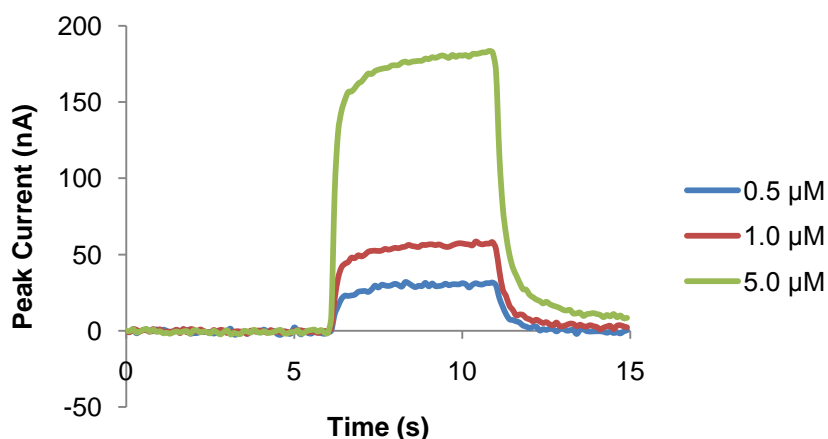


Figure 14. Peak currents (nA) of dopamine solutions of known concentrations in 10X PBS as observed in the flow cell as a function of time (s). The maximal peak current generated for each concentration was used for the calibration curve.

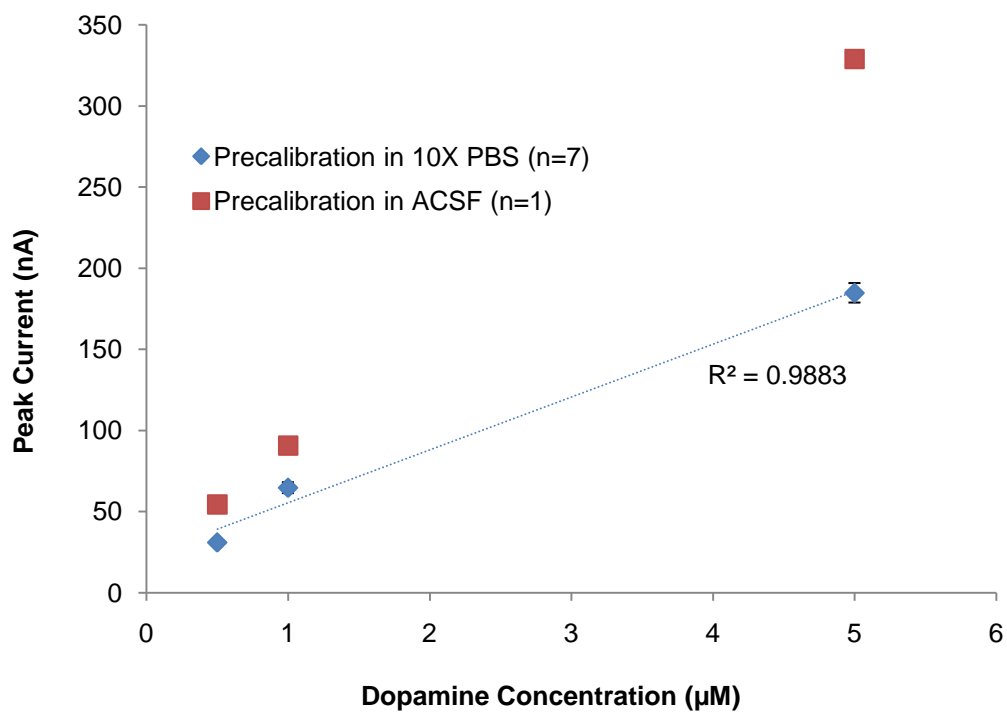
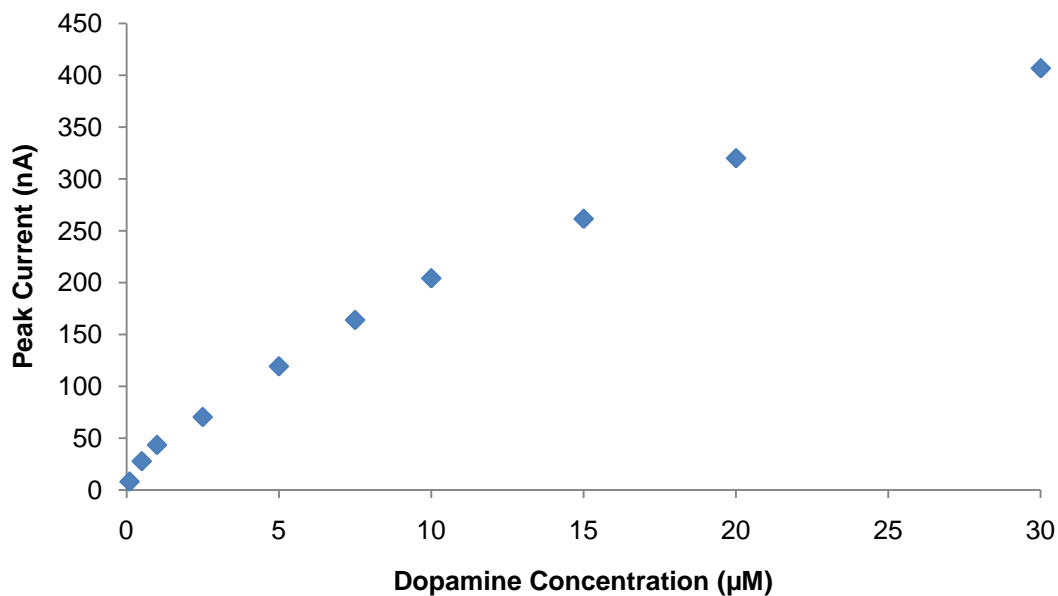
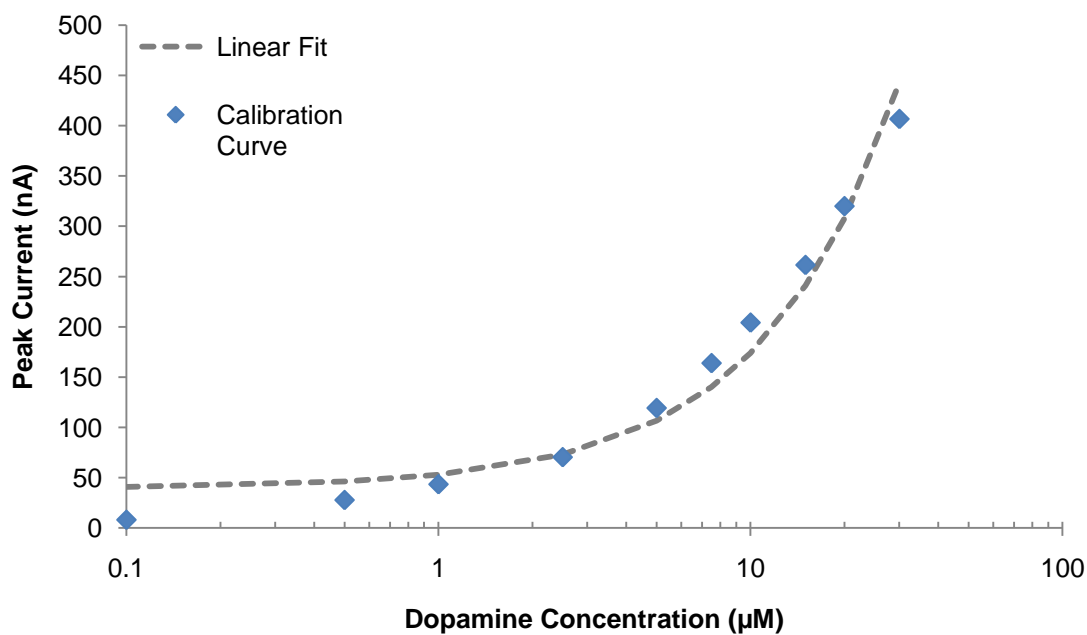


Figure 15. Calibration curve for electrochemical detection of dopamine in different solvents (error bars indicate standard error).



A.

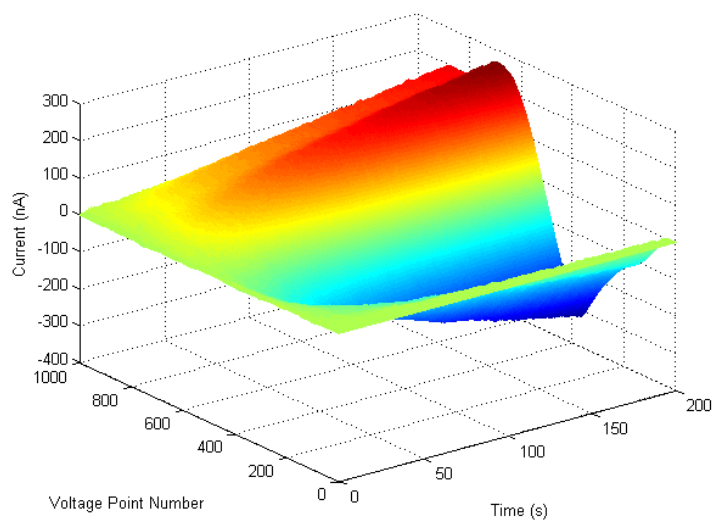


B.

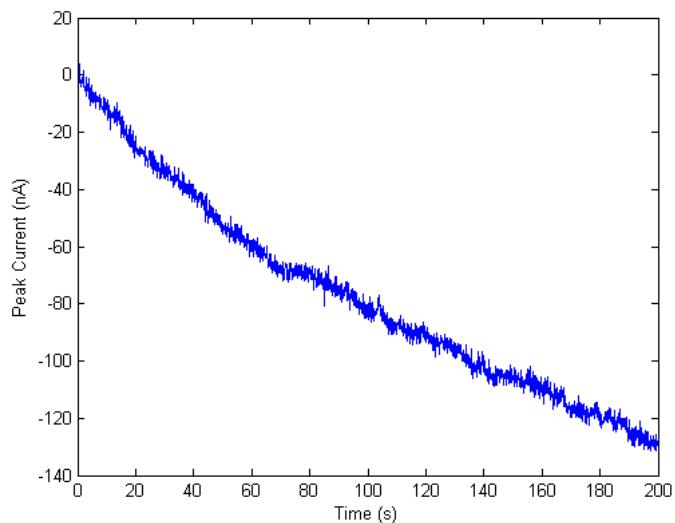
Figure 16. Calibration curves for electrochemical detection of dopamine displayed across a wide range of concentrations (A) and compared with a linear fit when plotted logarithmically (B).

3.1.2 Equilibration

Extensive equilibration behavior was observed as CFMEs reached steady state while continuously performing FSCV. The timescale necessary to reach state equilibria varied, but typically ran between 10 – 30 minutes. Decaying background current in the oxidation region and increasing current in the reduction region of the cyclic voltammogram were observed as characteristics of the equilibration process (Figure 17A). As the CFME equilibrated, the cyclic voltammogram became more stable over time. The threshold between the equilibration process of the electrode and the steady-state condition was defined as the point in time when observed background-subtracted peak current at +0.6 V did not exceed ± 2 nA over a 200 second period (Figure 18B).

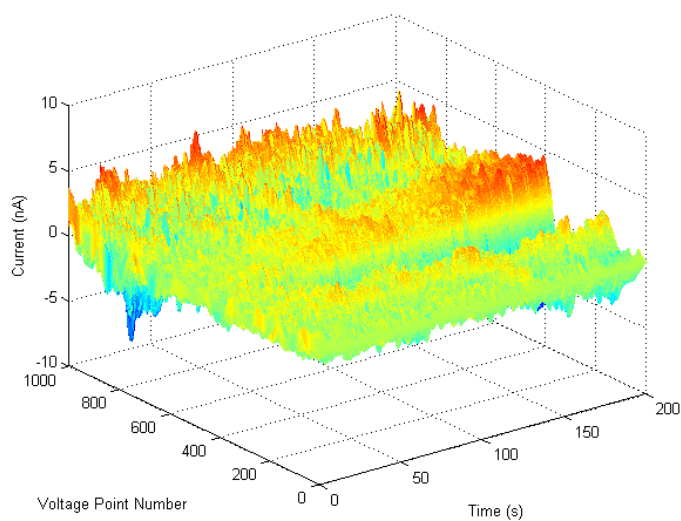


A.

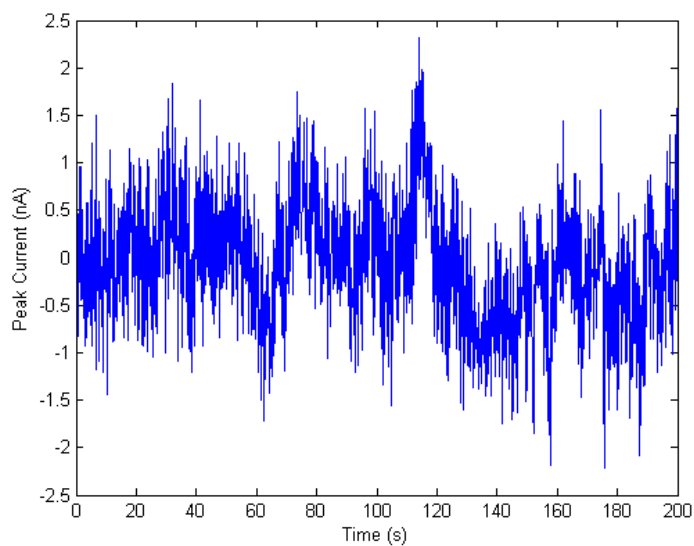


B.

Figure 17. (A) Dynamic background-subtracted cyclic voltammogram as the CFME equilibrated in 10X PBS. Voltage Point Number (VPN) indicates the potential of the CFME as a function of its point of progression in the voltage sweep. Each cycle is divided into 1000 increments as the voltage sweeps from 0 to +1.0 V, down to -0.5 V, and back to 0 V. (B) Decaying peak current at +0.6 V (VPN ~200), the characteristic oxidation potential of dopamine, from Fig. 17A as the CFME equilibrates over time.



A.



B.

Figure 18. (A) Dynamic background-subtracted cyclic voltammogram after the CFME has equilibrated to steady state. Note the difference in scale of the current (+z) axis between Figures 17A and 18A. (B) Steady-state peak current from Fig. 18A at +0.6 V, the characteristic oxidation potential of dopamine, as a function of time. The current does not exceed ± 2 nA.

3.2 Synthesis and Characterization of PPy/PSS/DA Electrodes

3.2.1 Electropolymerization of PPy/PSS Films

Constant current of 311 μA was applied to either the bare GCD electrodes or the GCD electrodes modified with the nanobead template, standardizing current density to 4.4 mA cm^{-2} . The voltage required to maintain the applied current was substantially higher for polymerization of PPy/PSS films through the nanobead template than for the same electrochemical process on bare GCD electrodes (Figure 19).

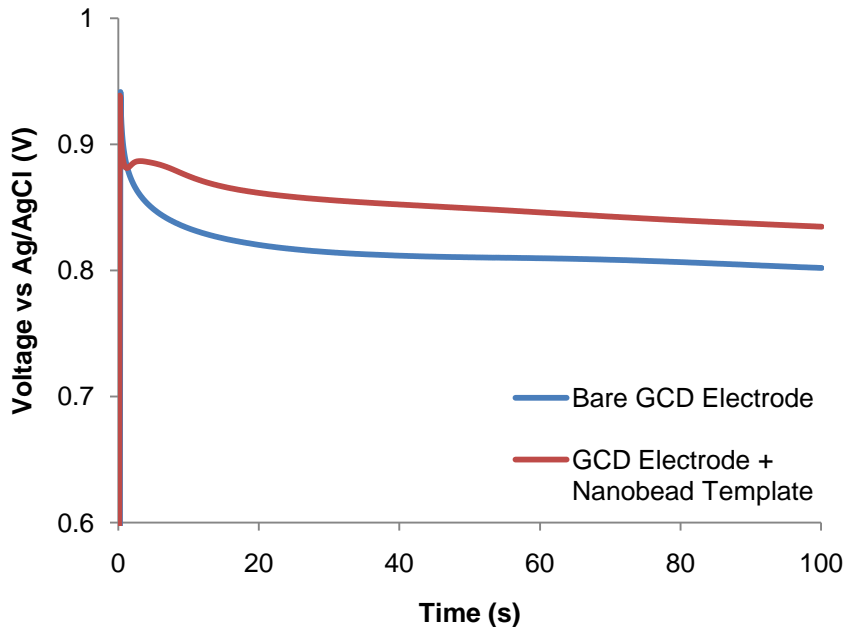


Figure 19. Average chronopotentiometric potential curves for electropolymerization of PPy/PSS films on bare GCD electrodes and GCD electrodes with a nanobead template (n=10 per group).

3.2.2 Redox Threshold and Stability of PPy/PSS

Cyclic voltammetry was performed on flat PPy/PSS films to test the stability of the polymer film and to confirm the position of the potentials at which oxidation and reduction of the film occur. The oxidation peak occurs slightly below 0 V, and the reduction peak appears most prominently at approximately -0.7 V. Many cycles of cyclic voltammetry were performed on the polymer film to test its stability over time and resilience to charging and discharging (Figure 20).

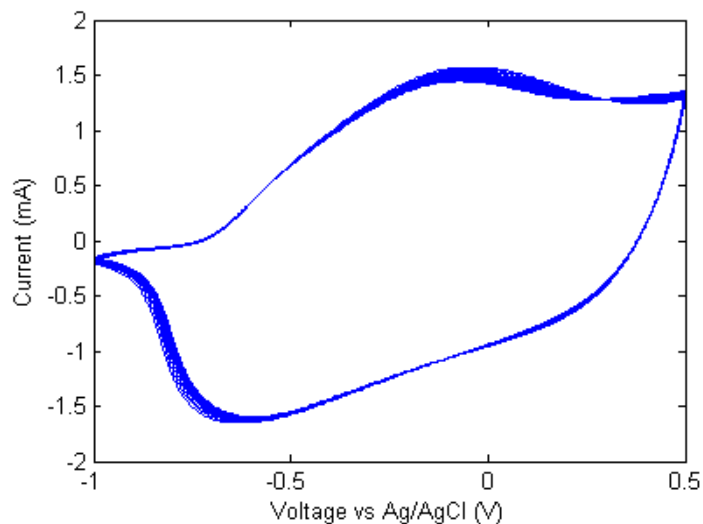


Figure 20. Cyclic voltammogram of flat PPy/PSS film on GCD electrode in 1X PBS solution using a three-electrode setup vs Ag/AgCl reference and platinum wire counter electrodes (scan rate = 100 mV/s). Several cycles are superimposed to depict the change in the response of the PPy/PSS film to repeated charging and discharging.

3.2.3 Cathodic Binding of Dopamine to PPy/PSS Films

Dopamine, positively charged in 10X PBS (pH ~7.4), was integrated into PPy/PSS films via a cathodic binding mechanism. Constant potential was applied at -0.6 V to the PPy/PSS modified electrode, incorporating dopamine into the conducting polymer structure (Figure 21).

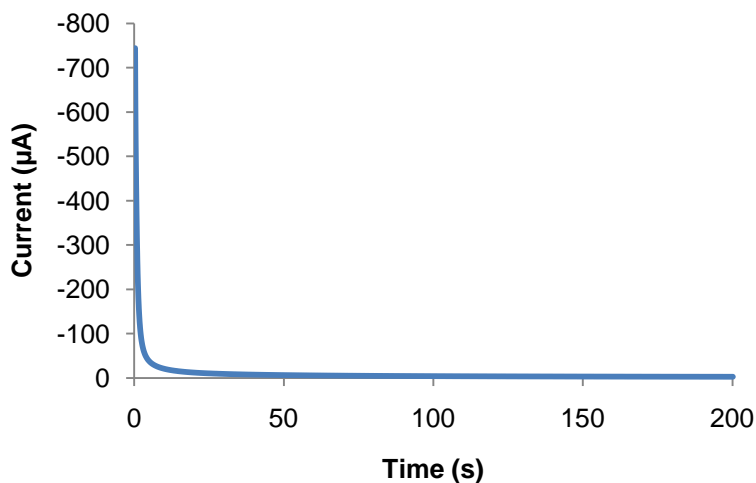


Figure 21. Amperometric decay as a function of time. Dopamine (0.1 M in deionized water) was cathodically bound to nanoporous PPy/PSS films by applying -0.6 V vs Ag/AgCl to the PPy/PSS modified electrodes for 200 seconds (n=10).

3.3 Effect of Electrical Release Stimulus on FSCV

The stimulus control was evaluated for both the flat PPy/PSS and nanoporous PPy/PSS modified electrode surfaces. This experiment serves as a control in which no dopamine is present anywhere in the system, and an electrical stimulus is applied to the PPy/PSS electrode in a similar fashion. The polymer-modified electrode was stimulated by switching its potential bias between -0.3 V, 0 V, and +0.3 V (Figure 22).

The bipotentiostat system allows for two simultaneous electrical stimuli to be applied to the same electrochemical system. The primary stimulation is the continuously sampling FSCV waveform, and the secondary stimulation is the electrical release stimulus indicated by the sharp current spikes (Fig. 22).

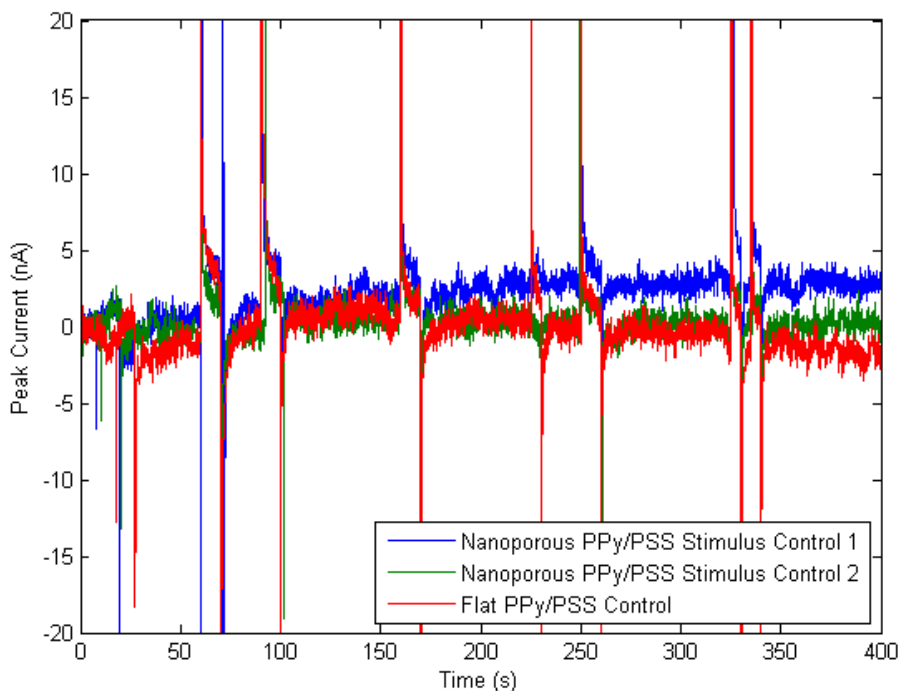
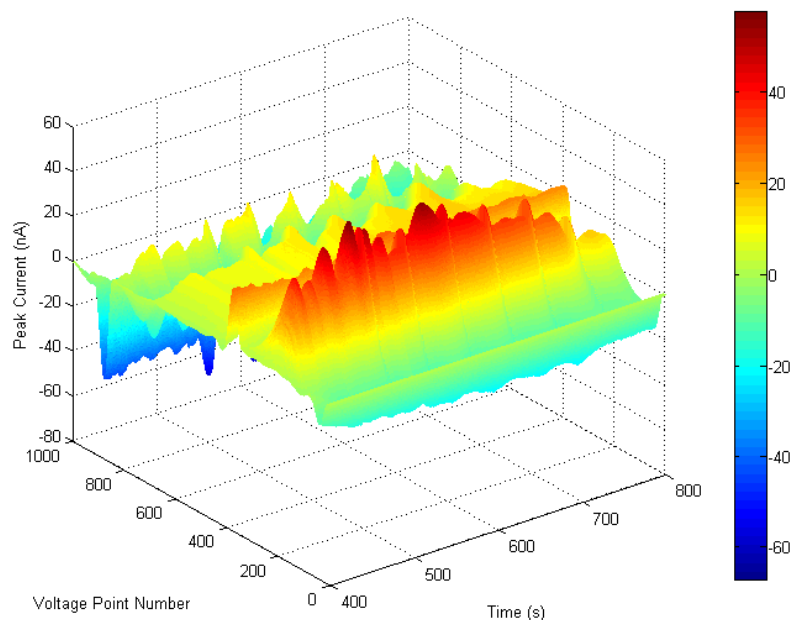


Figure 22. Dynamic peak current of CFME in 10X PBS over time with electrical stimulation. This is the stimulus control for nanoporous and flat PPy/PSS modified electrodes. Stimulation of the GCD electrodes suddenly changes the equilibrium of the solution, resulting in artifacts visible from the FSCV in the form of vertical lines.

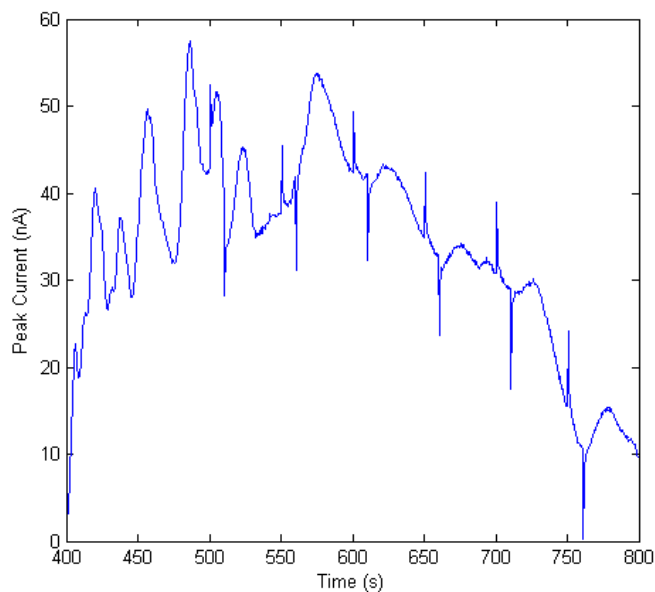
3.4 Controlled Dopamine Release from Flat PPy/PSS Films

Electrical pulses at +0.3 V triggered the release of dopamine from flat PPy/PSS films. The experimental setup was configured according to Fig. 13A, so the time starts at 400 seconds because the first half of the experiment required sampling a background

current without the PPy/PSS electrode present. Sampling for dopamine present in solution began at 400 seconds when 100 μ L of 1X PBS was added to the setup. Pulsatile electrical stimulation of the PPy/PSS modified electrode began at 500 seconds, and consisted of repeating intervals of 5 seconds of stimulation followed by 45 seconds of 0 V. Convective currents are observed in the first few minutes, and increases in dopamine-specific peak currents are observed following each stimulation artifact, immediately followed by a subsequent decrease in peak current (Figure 23). Overall, dopamine release from this electrically controlled system can be approximately quantified at 1.1 μ M (~17 ng in 100 μ L).



A.



B.

Figure 23. (A) Dynamic background-subtracted cyclic voltammogram of pulsatile dopamine release from flat PPy/PSS modified GCD electrodes. Dopamine oxidation was characterized at +0.634 V (VPN ~211), and peak current at this potential was plotted (B). To prepare this electrode, dopamine (0.05 M) was cathodically bound to PPy/PSS by applying constant voltage of -0.6 V for 100 seconds. Time starts at 400 seconds because the experimental setup was configured as described in Fig. 13A, requiring replacement of the platinum electrode used for background with the PPy/PSS/DA modified GCD electrode.

3.5 Dopamine Release from Uncapped Nanoporous PPy/PSS Films

3.5.1 Diffusion

Diffusion from PPy/PSS films, in the context of this thesis, can be described as the presence of dopamine in solution without an oxidative stimulus applied to the polymer film. In this sense, diffusion rather than electrochemical-mediation as a mode for release was seen from all PPy/PSS films in varying degrees. In uncapped nanoporous PPy/PSS films, dopamine release via diffusion was prevalent (Figure 24).

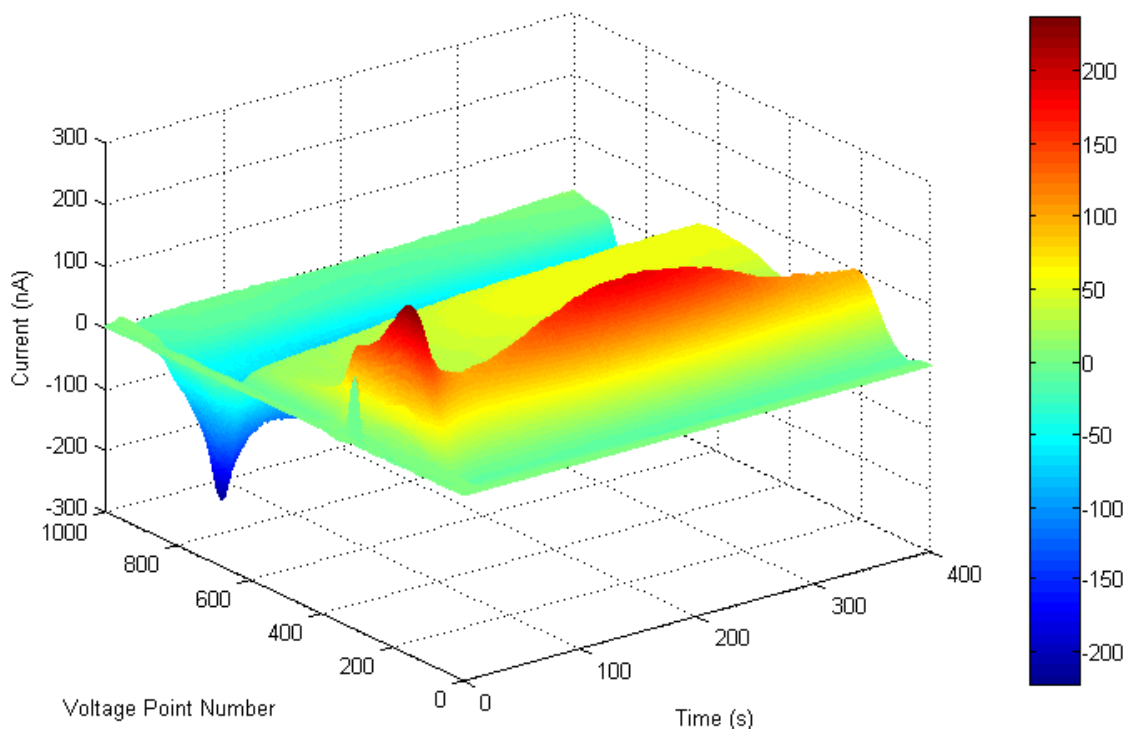


Figure 24. Dynamic background-subtracted cyclic voltammogram illustrating dopamine diffusion over time from a nanoporous PPy/PSS film. Dopamine oxidation peak current is identified by the contour of the maximal red crest, occurring at +0.631 V (VPN ~210). The PPy/PSS modified electrode held at a bias of 0 V vs Ag/AgCl.

Dopamine diffusion from nanoporous PPy/PSS films was analyzed when the polymer-modified electrode was held at a bias of -0.3 V vs Ag/AgCl. The solution was sampled with FSCV until the peak current reached an assumed plateau of equilibrium. Diffusion as a function of potential bias of the nanoporous PPy/PSS modified electrode was compared (Figure 25). Overall release of dopamine from diffusive mechanisms can be estimated at 2.1 μM and 5.3 μM (~ 64 ng and ~ 160 ng) for the polymers held at 0 V and -0.3 V respectively. Diffusion from the uncapped nanoporous PPy/PSS film at -0.3 V bias was analyzed a second time over a longer timescale. Peak currents were recorded until the release profile reached a plateau indicating steady state equilibrium. The dopamine released from the uncapped nanoporous polymer film via diffusion at -0.3 V bias is estimated at 4.5 μM (~ 138 ng).

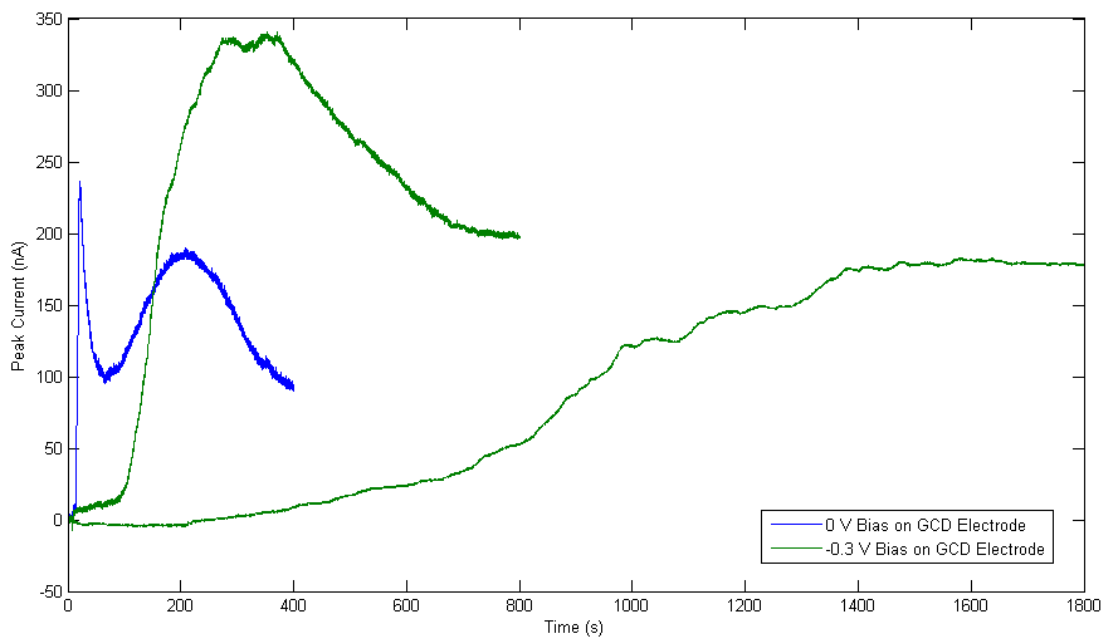


Figure 25. Peak current at dopamine oxidation potential detecting diffusion of dopamine from uncapped nanoporous PPy/PSS as a function of bias of the GCD electrode (n=1 for 0 V bias, n=2 for -0.3 V bias).

3.5.2 Electrically Controlled Release

Nanoporous PPy/PSS films loaded with dopamine were rinsed in 10X PBS for varied periods of time at a potential bias of either 0 V or -0.3 V vs Ag/AgCl. This is meant to encourage diffusion, or uncontrolled release, of any loosely adhered dopamine until it is no longer observed, thereby ensuring that dopamine remaining in the film to be released later is done so in a controllable fashion. The electrical stimulus controlling release was toggled from its potential bias to +0.3 V in a series of pulses. Dopamine release was observed after application of +0.3 V stimuli as evidenced by peak currents at the oxidation potential of dopamine that increased much more than the stimulus control (Figure 26).

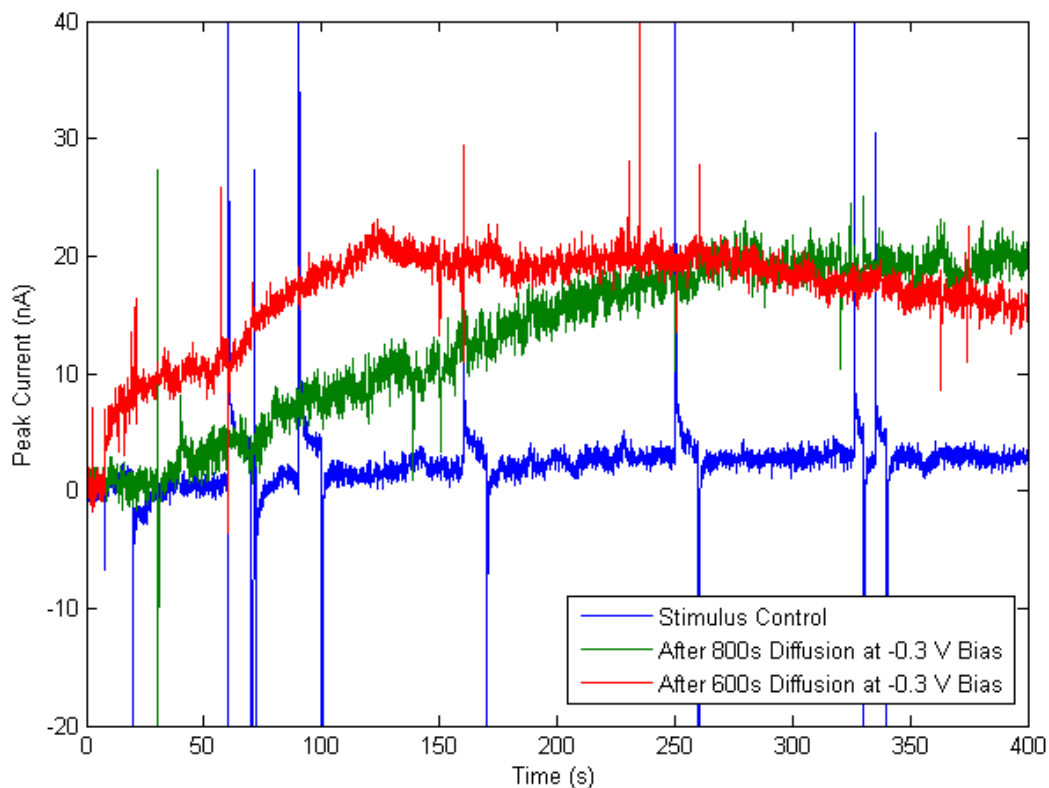


Figure 26. Dynamic profiles of dopamine peak currents vs time from nanoporous PPy/PSS films.

3.6 Dopamine Release from Capped Nanoporous PPy/PSS

Nanoporous PPy/PSS films were capped with an additional layer of PPy/PSS as described in section 2.2. In an effort to incorporate dopamine within the nanoporous structure of the capped nanoporous film, the GCD electrode was reduced to cathodically bind dopamine through the semi-permeable cap. Dopamine release from both diffusive and electrical mechanisms was quantified.

3.6.1 Diffusion

Dopamine diffusion from the capped nanoporous PPy/PSS film on GCD electrodes held at a -0.3 V bias was recorded until the peak current was observed to plateau at steady-state equilibrium. Dopamine diffusion from the capped nanoporous PPy/PSS film was estimated at 40.8 μM (~1250 ng). The peak current vs time plot is shown in Figure 27.

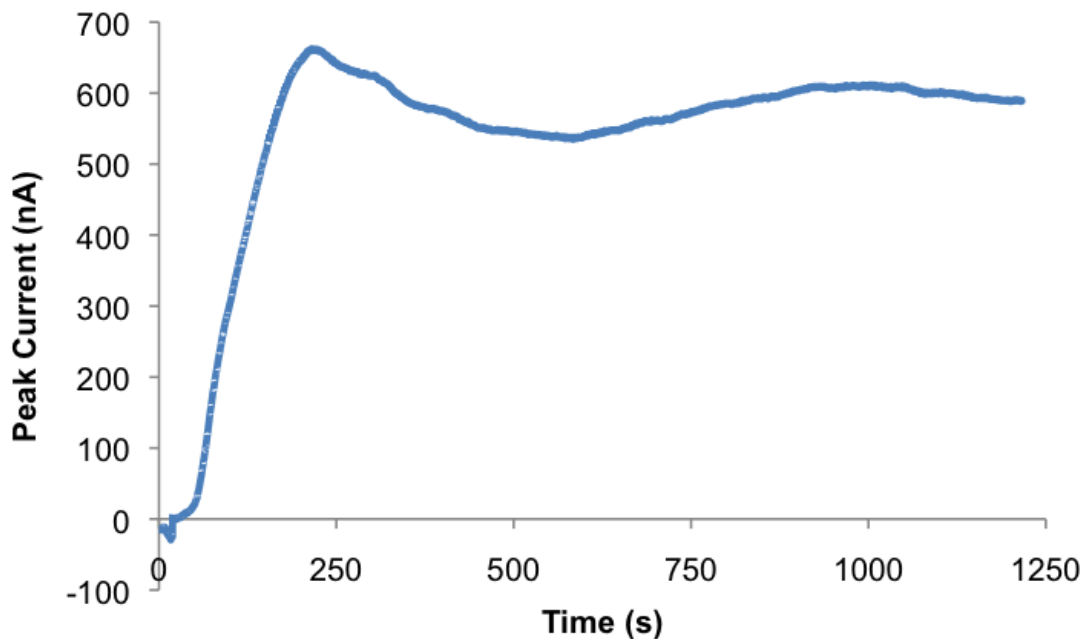


Figure 27. Peak current at dopamine oxidation potential to detect diffusion from nanoporous PPy/PSS films capped with an additional layer of PPy/PSS as a function of time.

3.6.2 Electrically Controlled Release

After dopamine release from diffusion subsided to steady state, the capped nanoporous PPy/PSS films with dopamine were subjected to pulses of +0.3 V as described in section 2.6. The resulting peak current vs time plot is shown in Figure 28.

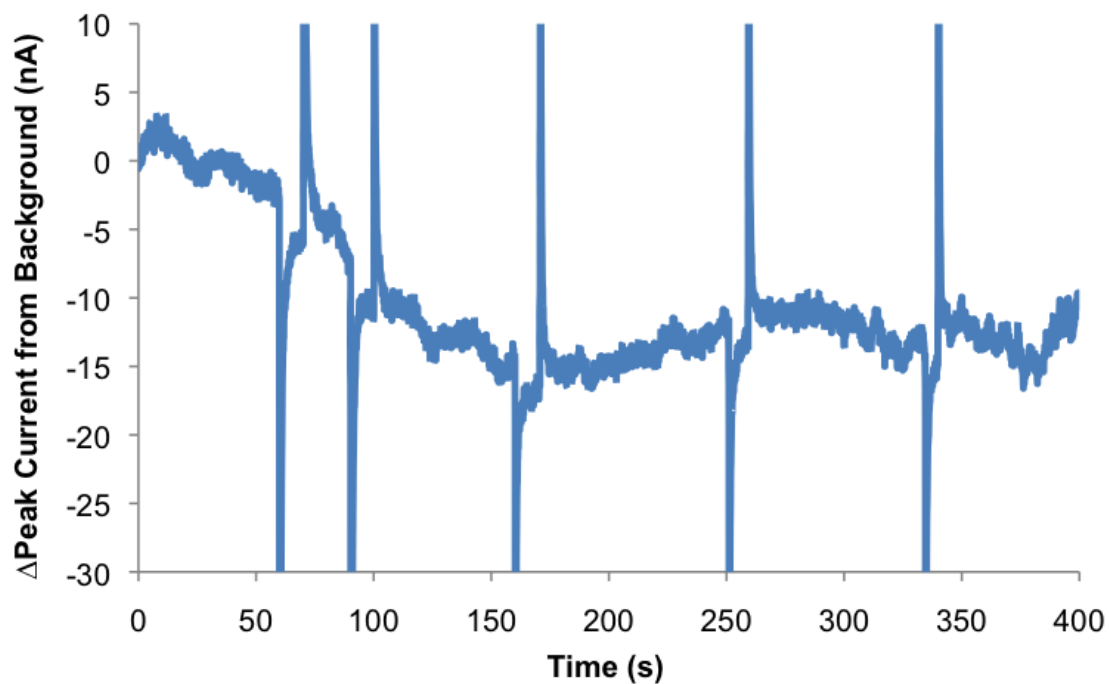


Figure 28. Change in peak current at dopamine oxidation potential as a function of time for capped nanoporous PPy/PSS film after diffusion. Background current was defined as the current recorded after dopamine diffusion in solution.

3.7 Summary of Dopamine Release from Polymer Films

Dopamine release from the various mechanisms described in the previous sections was quantified and compared as shown in Figure 29.

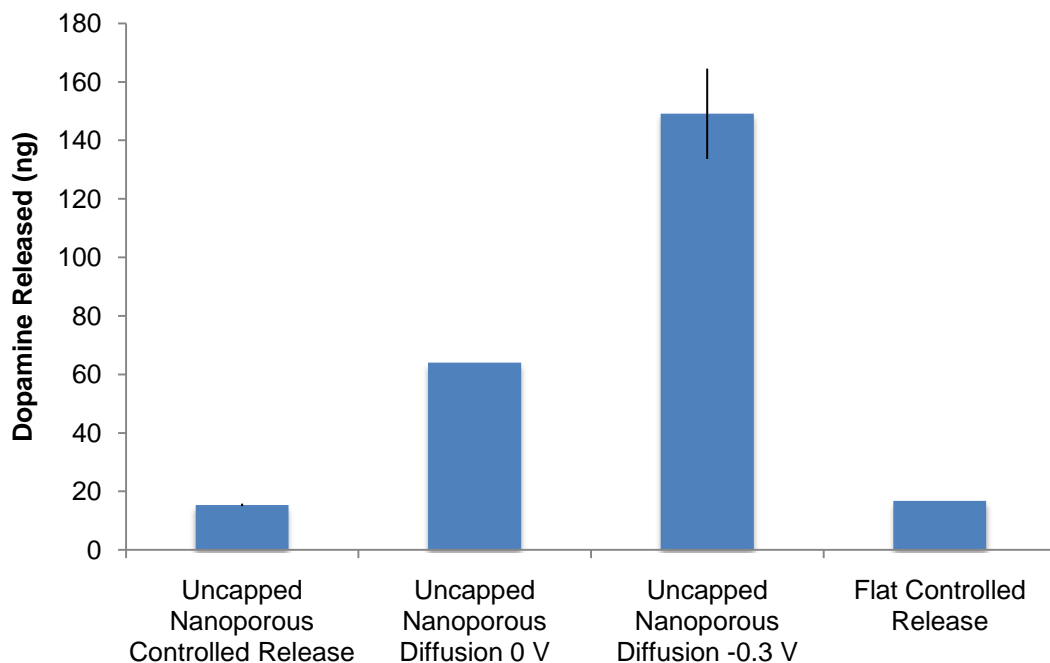


Figure 29. Dopamine release from the various substrate electrodes via diffusive and controlled release mechanisms. Diffusion from the capped nanoporous film at -0.3 V (not shown) released 1250 ng of dopamine. Error bars indicate standard deviation, sample size is $n=1$ for both uncapped nanoporous diffusion at 0 V and flat controlled release, and $n=2$ for both uncapped nanoporous controlled release and uncapped nanoporous diffusion at -0.3 V.

4.0 DISCUSSION

Successful controlled release of dopamine from conducting polymers offers a compelling opportunity for clinical treatment of neurological disorders. Even more promising is the applicability of this controlled release system to a wide range of pharmaceutical compounds of interest. Dopamine is inherently highly unstable, and successful characterization of its release from conducting polymers with its molecular structure intact suggests that the electrical release system will not affect the biological functionality of more resilient molecules.

At this point, it is clear that the original aims of this study have not been met in entirety. This project is intended to electrochemically bind and release dopamine from the conducting polymer while maximizing the carrying capacity, minimizing dopamine leaking out due to diffusion, and preserving the biological functionality of the released dopamine. Instead, the two polymer systems developed satisfy several of these aims to varying degrees.

4.1 Cathodic Binding of Dopamine

Dopamine binding to the conducting polymer films is a process that is theoretically plausible and has been verified experimentally [26, 27]. Experimental validation of this process runs in concert with verification of electrically controlled release. Quantification of changes in mass of the modified electrode surface during cathodic binding of dopamine was not performed. Therefore, it is assumed that the process of electrostatic binding of dopamine to the polymer film is a prerequisite to

controlled release, i.e. controlled release of dopamine cannot happen without it binding cathodically first. If this assumption is correct and no other interactions are responsible for controlled release of cationic drugs, these findings corroborate past experimental evidence.

Incorporation and release of cations from conducting polymers is mechanistically more complex than traditional doping that is seen in anionic drug release systems (Fig. 2,3). As such, the electrochemical process of loading cationic drugs into conducting polymers must sequentially follow electropolymerization of the polymer itself, whereas anionic drugs are loaded into the polymer film during its synthesis. The separation of these two processes offers a further degree of freedom in the customizability of a controlled release system, as well as another potential area for complications.

Typically the monomer and dopant concentrations, parameters of electropolymerization, and morphology of the substrate electrode have profound effects on the conductivity, actuation ability, and structure of the polymer film. These three polymer properties can significantly change the characteristics of drug release. Conductivity and surface area of the film are related to how effectively the polymer can charge and discharge and interact with the loaded drug to electrostatically drive its release. Actuation, or movement of the polymer, helps to drive drug release during its swelling and contracting with ionic flux.

In a cationic loading and releasing mechanism, the disconnection between the drug loading and polymer synthesis processes can lead to less intimate electrostatic interactions between the drug and the polymer compared to doping. However, the process of cathodic binding of the drug to the film offers another degree of freedom with the type

of electrochemical process used for loading. For example, slow cyclic voltammetry might prove to be more effective to load cationic drugs to conducting polymer films than constant current because of the repetitive pumping of the polymer that this method affords. Therefore, while the experimental evidence supports the notion that constant reductive potential binds dopamine to the polymer film, other electrochemical methods could result in more effective electrostatic interactions between the cationic drug and the polymer. This suggests that less dopamine would be released from diffusion, ultimately leading to a more controllable mechanism of release.

Cathodic binding of dopamine to the conducting polymer is a function of the redox capabilities of the polymer itself. In this study, the potential used to bind dopamine was -0.6 V, whereas the polymer was more fully reduced at a potential of -0.7 or -0.8 V as shown by the position of the reduction peak in the cyclic voltammogram of the PPy/PSS film (Fig 20). While dopamine was observed to cathodically bind to the polymer film, a possible reason for it to bind less completely is that the conducting polymer was not sufficiently reduced to fully drive electrostatic incorporation of dopamine into the film. This is one possible contributing factor to the high quantities of dopamine diffusion that are especially prevalent in the nanoporous structure.

4.2 Dopamine Release

The processes of diffusion and electrically controlled release are strongly connected to the amount of drug loaded into the film. Consequently, it is difficult to discuss the release processes as independent of the drug capacity of the polymer. As the structure implies, nanoporous polymer films have been shown to carry much more drug

than their non-nanoporous counterparts [19, 29]. However, this increased capacity also stems from a fundamentally different relationship between the loaded drug and the film than in the non-nanoporous case. While the electrostatic binding process occurs to incorporate dopamine into both polymer films, the data indicating extensive diffusion from the nanoporous films suggest more of a reservoir-type drug storage mechanism. Simply put, more dopamine can be stored in the nanoporous film because there is much more space for it to occupy. The added consequence of this nanoporous structure is that the dopamine leaks out almost as easily as it was incorporated (Fig. 25), leaving much less dopamine available for electrically controlled release (Fig. 26). In fact, while more dopamine was incorporated into the nanoporous film than the flat film, the amount of dopamine observed by controlled release was below the detection limit of the carbon-fiber microelectrode.

Diffusion at different potential biases from nanoporous PPy/PSS films yielded results that are, at first glance, counterintuitive to our understanding of the redox binding and release mechanism of conducting polymers. The conventional opinion of this mechanism for cationic drugs is that reduction of the polymer promotes binding and retention of drug in the film, and oxidation of the polymer triggers release. The expected result would therefore be dopamine diffusion from the polymer that is inhibited by lower potentials. Yet it is important to acknowledge that the degree of oxidation and reduction of the polymer is not linearly proportional to its potential bias. The oxidation and reduction peaks (Fig. 20) indicate the potentials at which oxidation and reduction are favored (approximately 0 V and -0.7 V respectively). With this in consideration, the diffusion observed from the polymer at 0 V bias should not be substantially more than

that observed from the polymer at -0.3 V. However, over twice as much dopamine was released from the nanoporous polymer held at -0.3 V than the nanoporous polymer at 0 V. This result is likely caused by experimental error and a more rational relationship will likely result from repeated trials.

The most intriguing aspect of these diffusion results at negative potential bias is the delay in drug release. It appears that holding the dopamine-bound electrode film at a negative potential inhibits the passive release of dopamine from the film (Fig. 25). In these two trials, dopamine was retained for 100-200 seconds before it started to leak out of the film. This offers a very promising direction for future research in controlled release. However, this retention of dopamine was not indefinite. After 100-200 seconds, dopamine began to diffuse from the polymer, the underlying reasons for which are currently unknown and must be investigated further. The variability in diffusion profiles observed from these two uncapped nanoporous films is probably due to differences in positioning of the CFME relative to the releasing electrode. Still, the overall effect is the same. Both electrodes exhibit a delay of dopamine diffusion, and both electrodes release very similar quantities of dopamine over the course of this diffusion process.

Substantially less diffusion of dopamine was observed from the release profile of the flat PPy/PSS films (Fig. 23B, 400-500s). Though this process was not tested thoroughly, repeating cycles of rising and falling peak currents are likely attributed to convective fluid flow within the droplet as the 1X PBS solution was added. This inability to effectively quantify diffusion was one of the shortcomings of the initial experimental configuration and motivating factors to reconfigure the setup (Fig. 13A). Still, electrically controlled release was observed after each applied stimulus (+0.3 V pulses), recognized

by a local increase and decrease in peak current after each stimulus. Long-term decay of peak current after several stimulations is explained by diffusion of the electrically released dopamine throughout the solution over time (Fig. 23B). The advantage of this setup is the minimal distance between the polymer-modified electrode and the CFME positioned 250 μm opposite its surface, providing highly responsive temporal resolution of release that is not reproduced by the other experimental configurations.

4.3 Dopamine Release from Capped Nanoporous Films

While the ultimate aim is to maximize controlled release while minimizing diffusion, it seems as though the opposite trend pervades the existing system of drug release based on nanoporous conducting polymers. One approach to minimizing the extensive diffusion without reducing the amount of dopamine loaded would be to incorporate a semipermeable cap. Electropolymerization of this cap poses additional challenges, but the electrochemical properties of the cap should mimic the behavior of the traditional, non-nanoporous polymer film in conductivity, permeability, and actuation.

The preliminary studies of dopamine incorporation and release from capped nanoporous films suggest a number of processes that are less than ideal for controlled release mechanisms. Several caps of different permeabilities for the nanoporous film were previously developed by varying the scan rate of electropolymerization, and drug release from these capped nanoporous films was studied. The most permeable cap was used for this thesis because it needed to allow dopamine to first pass from solution into the nanopores before it could be subsequently released from the nanopores, through the cap once more, and into solution. While prior research focuses on capping the

nanoporous film after the drug already incorporated into the nanopores [19, 29], this capping process would oxidize the bound dopamine into the quinone, rendering it physiologically irrelevant, described in greater detail in section 4.5.

The data from this type of electrode show extensive diffusion of dopamine that greatly exceeds drug release from any of the other polymer films, almost by a full order of magnitude (Fig 27, 29). After diffusion, the release profile from electrical stimuli shows not only a lack of dopamine release, but also a decay in peak current (Fig 28). These data are consistent with the expected behavior of the electrode if the dopamine never permeated the polymer cap in the first place. The extensive diffusion is likely the result of loose adhesion of dopamine cathodically bound to the outer layer of the polymer cap. Despite the implementation of the most permeable polymer cap, no dopamine release was observed upon application of the oxidative electrical command stimulus. The decrease in peak current observed from the pulse train is most probably attributed to either continued equilibration of the CFME, or continued diffusion of higher concentrations of dopamine from the region of the droplet with the electrodes to the outer edges.

This ineffective application of the polymer cap for dopamine release from nanoporous films can be approached several ways. First, further optimizing the permeability of the polymer cap should be possible by varying the parameters of its electrochemical synthesis. If that proves unsuccessful, polymer-based switches and gates could be implemented to physically permit or inhibit the release of dopamine from the electrode by implementing the unique property of electrically driven actuation for conducting polymers. Another possible solution would be to incorporate an active

reductant into the nanoporous polymer film with dopamine prior to capping. This would allow dopamine to be released with its structure preserved, due to the reductant becoming oxidized rather than dopamine.

4.4 Limitations of Experimental Setup

As explained previously, electrical release is governed by the oxidation and reduction of the polymer. The optimization of the electrical signal that causes this oxidation and reduction of the polymer backbone is therefore critical to designing the controllability of the release. In the current experimental setup, the electrical stimulus applied to the polymer-modified electrode is determined by flipping a toggle switch that applies a predetermined potential in either the anodic or cathodic direction. As such, the magnitude of the release stimulus is limited to this predetermined potential (in either direction) and the rest potential (0 V). The flexibility of the release stimulus is further constricted to voltage pulses as opposed to other electrical waveforms that may prove to be more effective in releasing dopamine from the polymer.

Accurate and reliable quantification of dopamine is absolutely critical for the successful execution of this project, especially for the low concentrations of dopamine that are relevant for this study and even lower concentrations that are clinically significant. Fast-scan cyclic voltammetry with carbon-fiber microelectrodes is the analytical method of choice for detection of dopamine and other catecholamines *in vivo*. For *in vitro* dopamine studies of this nature, however, other factors complicate this relatively straightforward electroanalytical method of analysis.

One issue that arose was the positive drifting of the oxidation potential where dopamine oxidation was observed within the same release (or diffusion) trial. Two potential causes of this are the superposition of a dynamic equilibration curve, and shifting solution pH. Since each trial of electrically controlled dopamine release requires many minutes of data recorded at 10 Hz, it is possible that the background curve of the CFME changed significantly over this period of time. Superposition of this changing background curve due to CFME equilibration (Fig. 17) on top of the actual dopamine signal could potentially cause the oxidation potential of dopamine to drift within a release trial. Therefore, ample time was given for the CFME to equilibrate to steady state beforehand (Fig 18). The other potential cause of peak shifting is a change in solution pH over the course of a release trial generated from the protons present in the characteristic redox reaction of dopamine (Fig. 6). The buffer solution was changed from 1X PBS to 10X PBS to better neutralize any acidic or basic byproducts.

Clinically relevant dopamine concentrations run several orders of magnitude smaller than the dopamine concentrations observed in this system. Additionally, calibration sensitivity of carbon-fiber microelectrodes for catecholamine detection has been shown to vary dramatically between solvents. The data suggest that carbon-fiber microelectrodes are less sensitive to dopamine in 10X PBS than in ACSF (Fig. 15). The same relationship is experimentally supported in the detection of other catecholamines using CFMEs as well [64]. While the concentrations of dopamine for this *in vitro* study are much higher than typical *in vivo* levels, the strong 10X PBS buffer that this experiment requires to avoid solution pH shifts may possibly be limiting the capacity of the electrode to detect dopamine. This is supported by the post-diffusion controlled

release data from the nanoporous films (Fig. 26). A dynamic increase in dopamine oxidation peak currents was observed while the net change (+20 nA) was still under the detection limit of that specific CFME when the dopamine calibration was fit to a linear curve.

Linearity may not be an appropriate assumption for the trend of peak currents versus dopamine concentrations for the range of calibration. The carbon surface substrate is highly conducive to dopamine adsorption, and this adsorption is supposed to increase dopamine sensitivity [65]. The sensitivity of the CFMEs can therefore be described as a function of dopamine adsorption. Calibration of the CFMEs to standardize peak currents to dopamine concentrations served the secondary purpose of pre-exposing the CFMEs to dopamine prior to release quantification. Pre-exposure of the CFMEs to dopamine is designed to control dopamine adsorption to a stable level. This thereby ensures a stable calibration that is less significantly altered by the presence of dopamine from the controlled release system. While linear relationships are generally used to calibrate CFMEs for the dopamine detection, it is essential that the range of calibration concentrations include the entire range of dopamine concentrations that are observed while detecting dopamine release in this system. Dopamine adsorption alters this calibration curve. The accuracy of the calibrated fit against the expected theoretical relationship between concentration and peak current has yet to be explored.

Another potential source of complication for the CFME arises from inserting a large disk electrode into a system typically used for CFMEs alone. When the potential of the PPy/PSS modified GCD electrode changes, a spike in the cyclic voltammogram of the CFME is observed. While this phenomenon has consistently been referred to as an

“artifact,” this term is not entirely accurate. Labeling this as an artifact implies that there is some glitch in the bipotentiostat or data analysis equipment that falsely provided graphical representation of an event that actually did not occur, when this is simply not the case. The spike is the response of the CFME to the sudden change in current that such a comparably large electrode imparts onto the system. Practically, these spikes serve as visual markers to indicate the temporal location of the electrical release stimulus. Subjecting the CFME to frequent stimuli of high current could potentially alter its long-term performance. However, the CFME seems unaffected in the short term and there is nothing to suggest this mode of electrode failure without further experimentation.

4.5 Limitations with Dopamine

The development of a conducting polymer system for dopamine release has been a process riddled with complexities. The chemical instability of dopamine has consequences that are both beneficial and challenging to this research. It is readily oxidized to dopamine-*o*-quinone, and fast-scan cyclic voltammetry capitalizes on the fast kinetics of this reaction, making electrochemical detection of dopamine very feasible. However, oxidation of dopamine otherwise causes a multitude of challenges.

Autoxidation and autopolymerization of dopamine are processes that potentially complicate the incorporation within and release from conducting polymer films. Dopamine autoxidation is the first step to autopolymerization, in which dopamine reacts with molecular oxygen naturally in solution to ultimately form aggregates and precipitate out of solution. To inhibit this rapid process, dopamine solutions were kept under N₂ for the period of time after they were mixed prior to use. However, it is unknown how much

of this reaction occurs before dopamine can be cathodically bound. It is assumed that dopamine rather than any of its oxidized products is incorporated into the conducting polymer film, verified by the position of the oxidation and reduction peaks observed on FSCV. Dopamine, readily oxidized in solution, may also have a significant fraction of its concentration existing as the quinone during release studies. If more dopamine exists as the quinone, the oxidation peak would not be as high as the reduction peak, and detection sensitivity would be decreased using the peak current at the oxidation potential.

Another limitation of working with dopamine is the restrictions its instability imposes on the possible stimuli for the conducting polymer film. Dopamine typically oxidizes between +0.5 and +0.7 V. To retain the molecular structure and biological functionality of dopamine, the potential of the polymer should not approach these values where dopamine oxidation would render it biologically useless and potentially even toxic [43]. The potential of the electrical release stimulus was predetermined not to exceed +0.3 V to avoid this process.

This has three implications on the behavior of the polymer. First, it does not allow for higher degrees of actuation of the polymer that higher potentials would cause, limiting the ability of the polymer to expand and contract to more effectively engage in ion exchange and subsequent dopamine release. Second, the slight +0.3 V potential may still be high enough to promote autopolymerization within the polymer film. Autopolymerization and aggregation of dopamine within the polymer film would drastically reduce the amount of dopamine available to release and inhibit the release of the dopamine that is available. Finally, electropolymerization of semipermeable polymer caps over nanoporous PPy/PSS/DA films to inhibit diffusion is no longer a feasible

option due to the sensitivity of dopamine to oxidative stimuli. Initiation of electropolymerization is typically done with potentials upwards of +0.7 V vs Ag/AgCl, which would oxidize dopamine contained within the film to the quinone. Therefore, capping the nanoporous conducting polymer film would have to precede cathodic binding of dopamine. The permeability of the cap would have to be optimal to allow dopamine to be pulled through in the binding process, but prevent excessive diffusion in the release process.

5.0 CONCLUSIONS AND FUTURE WORK

Electroactive conducting polymer films hold promise for the development of customizable, controllable drug release systems. The advantage of a nanoporous structure over a non-nanoporous structure of conducting polymers for electrically controlled dopamine release is greatly increased loading capacity. The primary mechanism of release was largely diffusion without any electrical stimulus, but electrically controlled release was observed in both flat and nanoporous conducting polymer films. Application of a reducing potential did not inhibit dopamine diffusion from the nanoporous polymer film.

Future work will focus on the development and optimization of the semi-permeable cap to inhibit dopamine diffusion from the nanoporous film and mediate electrically controlled release. Higher resolution and wider range of concentrations for calibration of the carbon-fiber microelectrodes will be investigated. While electrically controlled release of dopamine was observed, further experimentation to minimize diffusion and maximize controllability must be explored.

REFERENCES

1. Wallace, G.G., et al., *Conductive Electroactive Polymers: intelligent materials systems*. 2003, Boca Raton, FL: CRC Press.
2. Sadki, S., et al., *The mechanisms of pyrrole electropolymerization*. Chem Soc Rev, 2000. **29**: p. 283-293.
3. John, R. and G.G. Wallace, *The use of microelectrodes to probe the electropolymerization mechanism of heterocyclic conducting polymers*. J Electroanal Chem, 1991. **306**: p. 157-167.
4. Stauffer, W.R., *Manipulating and Understanding the Cultured Neuronal Network through Conducting Polymers*, in *Department of Bioengineering*. 2008, University of Pittsburgh: Pittsburgh, PA. p. 139.
5. Garner, B., et al., *Polypyrrole-heparin composites as stimulus-responsive substrates for endothelial cell growth*. J Biomed Mater Res, 1999. **44**(2): p. 121-9.
6. Garner, B., et al., *Human endothelial cell attachment to and growth on polypyrrole-heparin is vitronectin dependent*. J Mater Sci Mater Med, 1999. **10**(1): p. 19-27.
7. Collier, J.H., et al., *Synthesis and characterization of polypyrrole-hyaluronic acid composite biomaterials for tissue engineering applications*. J Biomed Mater Res, 2000. **50**(4): p. 574-84.
8. Cui, X., et al., *Surface modification of neural recording electrodes with conducting polymer/biomolecule blends*. J Biomed Mater Res, 2001. **56**(2): p. 261-72.

9. Stauffer, W.R. and X.T. Cui, *Polypyrrole doped with 2 peptide sequences from laminin*. *Biomaterials*, 2006. **27**(11): p. 2405-13.
10. Abidian, M.R., D.-H. Kim, and D.C. Martin, *Conducting-Polymer Nanotubes for Controlled Drug Release*. *Adv Mater*, 2006. **18**(4): p. 405-9.
11. Ateh, D.D., H.A. Navsaria, and P. Vadgama, *Polypyrrole-based conducting polymers and interactions with biological tissues*. *J R Soc Interface*, 2006. **3**(11): p. 741-52.
12. Cen, L., et al., *Assessment of in vitro bioactivity of hyaluronic acid and sulfated hyaluronic acid functionalized electroactive polymer*. *Biomacromolecules*, 2004. **5**(6): p. 2238-46.
13. Guimard, N.K., N. Gomez, and C.E. Schmidt, *Conducting polymers in biomedical engineering*. *Prog Polym Sci*, 2007. **32**(8-9): p. 876-921.
14. Cui, X., et al., *Electrochemical deposition and characterization of conducting polymer polypyrrole/PSS on multichannel neural probes*. *Sensor Actuat A-Phys*, 2001. **93**: p. 8-18.
15. Evans, A.J., et al., *Promoting neurite outgrowth from spiral ganglion neuron explants using polypyrrole/BDNF-coated electrodes*. *J Biomed Mater Res A*, 2009. **91**(1): p. 241-50.
16. Richardson, R.T., et al., *The effect of polypyrrole with incorporated neurotrophin-3 on the promotion of neurite outgrowth from auditory neurons*. *Biomaterials*, 2007. **28**(3): p. 513-23.
17. Richardson, R.T., et al., *Polypyrrole-coated electrodes for the delivery of charge and neurotrophins to cochlear neurons*. *Biomaterials*, 2009. **30**(13): p. 2614-24.

18. Wadhwa, R., C.F. Lagenaur, and X.T. Cui, *Electrochemically controlled release of dexamethasone from conducting polymer polypyrrole coated electrode*. *J Control Release*, 2006. **110**(3): p. 531-41.
19. Luo, X. and X.T. Cui, *Electrochemically controlled release based on nanoporous conducting polymers*. *Electrochem Commun*, 2009. **11**(2): p. 402-404.
20. Miller, L.L., B. Zinger, and Q.-X. Zhou, *Electrically controlled release of hexacyanoferrate(4-) from polypyrrole*. *J Am Chem Soc*, 1987. **109**(8): p. 2267-2272.
21. Zinger, B. and L.L. Miller, *Timed release of chemicals from polypyrrole films*. *J Am Chem Soc*, 1984. **106**(22): p. 6861-6863.
22. Kontturi, K., P. Pentti, and G. Sundholm, *Polypyrrole as a model membrane for drug delivery*. *J Electroanal Chem*, 1998. **453**(1-2): p. 231-238.
23. Pernaut, J.-M. and J.R. Reynolds, *Use of Conducting Electroactive Polymers for Drug Delivery and Sensing of Bioactive Molecules. A Redox Chemistry Approach*. *J Phys Chem B*, 2000. **104**(17): p. 4080-4090.
24. Pyo, M., et al., *Controlled release of biological molecules from conducting polymer modified electrodes : The potential dependent release of adenosine 5'-triphosphate from poly(pyrrole adenosine 5'-triphosphate) films*. *J Electroanal Chem*, 1994. **368**(1-2): p. 329-332.
25. Hepel, M. and F. Mahdavi, *Application of the Electrochemical Quartz Crystal Microbalance for Electrochemically Controlled Binding and Release of Chlorpromazine from Conductive Polymer Matrix* *Microchemical Journal*, 1997. **56**(1): p. 54-64.

26. Miller, L.L. and Q.X. Zhou, *Poly(N-methylpyrrolylium) Poly(styrenesulfonate). A Conductive, Electrically Switchable Cation Exchanger That Cathodically Binds and Anodically Releases Dopamine*. *Macromolecules*, 1987. **20**: p. 1594-1597.
27. Zhou, Q.-X., L.L. Miller, and J.R. Valentine, *Electrochemically controlled binding and release of protonated dimethyldopamine and other cations from poly(N-methyl-pyrrole)/polyanion composite redox polymers* *J Electroanal Chem*, 1989. **261**(1): p. 147-164.
28. Freedman, M.S. and X.T. Cui, *Substrate Electrode Morphology Affects Electrically Controlled Drug Release from Electrodeposited Polypyrrole Films*. 2010, University of Pittsburgh: Pittsburgh, PA.
29. Luo, X. and X.T. Cui, *Sponge-like nanostructured conducting polymers for electrically controlled drug release*. *Electrochem Commun*, 2009. **11**: p. 1956-1959.
30. Stone, T.W., *CNS Neurotransmitters and Neuromodulators: Dopamine*. 1996, Boca Raton, FL: CRC Press.
31. Dunnett, S.B., et al., *Dopamine*. *Handbook of Chemical Neuroanatomy*, ed. A. Björklund and T. Hökfelt. Vol. 21. 2005, Amsterdam, The Netherlands: Elsevier.
32. Hurd, Y.L. and H. Hall, *Human forebrain dopamine systems: Characterization of the normal brain and in relation to psychiatric disorders*, in *Dopamine*, S.B. Dunnett, et al., Editors. 2005, Elsevier: Amsterdam, The Netherlands.
33. Kim, K.C. and A. Burkman, *Dopaminergic Influences on Prolactin Synthesis and Release from Rat Anterior Pituitary Cultures*. *Arch Pharm Res*, 1980. **3**(2): p. 85-86.

34. Lookingland, K.J. and K.E. Moore, *Functional neuroanatomy of hypothalamic dopaminergic neuroendocrine systems*, in *Dopamine*, S.B. Dunnett, et al., Editors. 2005, Elsevier: Amsterdam, The Netherlands.
35. Meguid, M.M., et al., *Hypothalamic Dopamine and Serotonin in the Regulation of Food Intake*. *Nutrition*, 2000. **16**: p. 843-857.
36. *Catecholamines Biosynthesis*. [cited 2010 March 3, 2010]; Available from: http://en.wikipedia.org/wiki/File:Catecholamines_biosynthesis.svg.
37. Land, E.J., C.A. Ramsden, and P.A. Riley, *ortho-Quinone amines and derivatives: the influence of structure on the rates and modes of intramolecular reaction*. *ARKIVOC*, 2007(xi): p. 23-36.
38. Fausto, R., M.J. Ribeiro, and J.J.P. de Lima, *A molecular orbital study on the conformational properties of dopamine [1,2-benzenediol-4(2-aminoethyl)] and dopamine cation*. *Journal of Molecular Structure*, 1999. **484**: p. 181-196.
39. Graham, D.G., *Oxidative Pathways for Catecholamines in the Genesis of Neuromelanin and Cytotoxic Quinones*. *Molecular Pharmacology*, 1978. **14**: p. 633-643.
40. Klegeris, A., L.G. Korkina, and S.A. Greenfield, *Autoxidation of dopamine: a comparison of luminescent and spectrophotometric detection in basic solutions*. *Free Radical Biology & Medicine*, 1995. **18**(2): p. 215-222.
41. Smythies, J. and L. Galzigna, *The oxidative metabolism of catecholamines in the brain: a review*. *Biochimica et Biophysica Acta*, 1998. **1380**: p. 159-162.
42. Matsunaga, J., et al., *Biosynthesis of neuromelanin and melanin: the potential involvement of macrophage inhibitory factor and dopachrome tautomerase as*

- rescue enzymes*, in *Catecholamine Research: From Molecular Insights to Clinical Medicine*, T. Nagatsu, et al., Editors. 2002, Kluwer Academic/Plenum Publishers: New York, NY.
43. Graham, D.G., et al., *Autoxidation versus Covalent Binding of Quinones as the Mechanism of Toxicity of Dopamine, 6-Hydroxydopamine, and Related Compounds toward C1300 Neuroblastoma Cells in Vitro*. *Molecular Pharmacology*, 1978. **14**: p. 644-653.
 44. Cadet, J.L. and C. Brannock, *Free radicals and the pathobiology of brain dopamine systems*. *Neurochemistry International*, 1998. **32**: p. 117-131.
 45. Bragulat, V., et al., *Dopaminergic function in depressed patients with affective flattening or with impulsivity: [18F]Fluoro-L-dopa positron emission tomography study with voxel-based analysis*. *Psychiatry Research: Neuroimaging*, 2007. **154**: p. 115-124.
 46. Brown, A.S. and S. Gershon, *Dopamine and Depression*. *J Neural Transm*, 1993. **91**: p. 75-109.
 47. Lotharius, J. and P. Brundin, *Pathogenesis of Parkinson's disease: dopamine, vesicles, and α -synuclein*. *Nature Reviews: Neuroscience*, 2002. **3**: p. 1-11.
 48. Starr, M.S., *The role of dopamine in epilepsy*. *Synapse*, 1996. **22**: p. 159-194.
 49. Olanow, C.W., J.A. Obeso, and F. Stocchi, *Continuous dopamine-receptor treatment of Parkinson's disease: scientific rationale and clinical implications*. *Lancet Neurology*, 2006. **5**(8): p. 677-687.
 50. Barbeau, A., *L-Dopa Therapy in Parkinson's Disease: A Critical Review of Nine Year's Experience*. *Can Med Assoc J*, 1969. **101**(13): p. 59-68.

51. Group, T.P.S., *Levodopa and the Progression of Parkinson's Disease*. The New England Journal of Medicine, 2004. **351**(24): p. 2498-2508.
52. Benabid, A.L., *Deep brain stimulation for Parkinson's Disease*. Current Opinion in Neurobiology, 2003. **13**: p. 696-706.
53. Benabid, A.L., et al., *Deep brain stimulation of the corpus luyisi (subthalamic nucleus) and other targets in Parkinson's disease. Extension to new indications such as dystonia and epilepsy*. J Neurol, 2001. **248** [Suppl 3]: p. III/37-III/47.
54. Loddenkemper, T., et al., *Deep Brain Stimulation in Epilepsy*. Journal of Clinical Neurophysiology, 2001. **18**(6): p. 514-532.
55. Bard, A.J. and L.R. Faulkner, *Electrochemical Methods: Fundamentals and Applications*. 2001, Hoboken, NJ: John Wiley & Sons.
56. Justice, J.B.J., A.C. Michael, and D.B. Neill, *In Vivo Voltammetry*, in *Neuromethods: Amines and Their Metabolites*, A.A. Boulton and G.B. Baker, Editors. 1985, Humana Press: Clifton, NJ.
57. Philips, P.E.M. and R.M. Wightman, *Critical guidelines for validation of the selectivity of in-vivo chemical microsensors*. Trends in Analytical Chemistry, 2003. **22**(9): p. 509-514.
58. Scholz, F., *Electroanalytical Methods: Guide to Experiments and Applications*. 2002, Heidelberg, Germany: Springer-Verlag.
59. Brett, C.M. and A.M.O. Brett, *Electrochemistry: Principles, Methods, and Applications*. 1993, New York, NY: Oxford University Press.
60. Wightman, R.M., *Voltammetry with Microscopic Electrodes in New Domains*. Science, 1988. **240**: p. 415-420.

61. Garris, P.A. and R.M. Wightman, *Regional Differences in Dopamine Release, Uptake, and Diffusion Measured by Fast-Scan Cyclic Voltammetry*, in *Neuromethods: Voltammetric Methods in Brain Systems*, A.A. Boulton, G.B. Baker, and R.N. Adams, Editors. 1995, Humana Press: Totowa, NJ.
62. Wiedemann, D.J., et al., *Strategies for Low Detection Limit Measurements with Cyclic Voltammetry*. *Analytical Chemistry*, 1991. **63**(24): p. 2965-2970.
63. Moquin, K.F. and A.C. Michael, *Tonic autoinhibition contributes to the heterogeneity of evoked dopamine release in the rat striatum*. *J Neurochem*, 2009. **110**: p. 1491-1501.
64. Chen, B.T. and M.E. Rice, *Calibration Factors for Cationic and Anionic Neurochemicals at Carbon-Fiber Microelectrodes are Oppositely Affected by the Presence of Ca²⁺ and Mg²⁺*. *Electroanalysis*, 1999. **11**(5): p. 344-348.
65. Bath, B.D., et al., *Dopamine Adsorption at Surface Modified Carbon-Fiber Electrodes*. *Langmuir*, 2001. **17**(22): p. 7032-7039.